

Copy  
RM E50J30

NACA RM E50J30

E 50 J 30

0143210



TECH LIBRARY KAFB, NM

**NACA**

# RESEARCH MEMORANDUM

694

FORCE AND PRESSURE CHARACTERISTICS FOR A SERIES OF NOSE  
INLETS AT MACH NUMBERS FROM 1.59 TO 1.99

III - CONICAL-SPIKE ALL-EXTERNAL-COMPRESSION INLET  
WITH SUPERSONIC COWL LIP

By Maynard I. Weinstein and Joseph Davids

Lewis Flight Propulsion Laboratory  
Cleveland, Ohio

This document contains neither recommendations nor conclusions of the National Defense of the United States within the meaning of the Espionage Act, USC, 18:77 and 79. It is the property of the National Defense of the United States and is loaned to an employee or contractor by reason of his position. It is understood that its contents in any manner to be used for purposes other than those for which it was loaned, or to be given to any person not so loaned, may subject the individual to prosecution under the Espionage Act of 1917, as amended, or other appropriate laws.

**NATIONAL ADVISORY COMMITTEE  
FOR AERONAUTICS**

WASHINGTON  
February 14, 1951

319.98/13



0143210

1

NACA RM E50J30

1  
2039

## NATIONAL ADVISORY COMMITTEE FOR AERONAUTICS

RESEARCH MEMORANDUMFORCE AND PRESSURE CHARACTERISTICS FOR A SERIES OF  
NOSE INLETS AT MACH NUMBERS  
FROM 1.59 TO 1.99III - CONICAL-SPIKE ALL-EXTERNAL-COMPRESSION INLET  
WITH SUPERSONIC COWL LIP

By Maynard I. Weinstein and Joseph Davids

## SUMMARY

An investigation was conducted in the NACA Lewis 8- by 6-foot supersonic wind tunnel to determine the force and pressure characteristics of an all-external compression inlet having a conical spike and a supersonic cowl lip. Measurements of lift, drag, pitching moment, and internal and external pressures were made at free-stream Mach numbers of 1.59, 1.79, and 1.99 for a range of mass-flow ratios and angles of attack to  $10^{\circ}$ . The average Reynolds number based on inlet diameter was 2,300,000.

The drag increased rapidly with decreasing mass flow as a consequence of the increase in additive drag. The drag rise due to angle of attack resulted primarily from an increase in the normal force. At zero angle of attack, adequate theoretical predictions were made of the additive drag, friction drag, and at shock-swallowed conditions, the pressure drag.

The total-pressure recovery was in general only slightly reduced by increases in angle of attack to  $10^{\circ}$ .

## INTRODUCTION

A general study of the aerodynamic characteristics of a series of nose inlets suitable for supersonic ram-jet engines was conducted in the Lewis 8- by 6-foot supersonic wind tunnel. This report presents

the results of an investigation of a conical-spike inlet designed to give all-external compression and having a supersonic cowl lip. The performance of two other inlets is discussed in references 1 and 2.

The purpose of the investigation was to obtain force, moment, and pressure data, and when possible to compare the experimental results with theory. Data were obtained for a range of mass-flow ratios and angles of attack at free-stream Mach numbers 1.59, 1.79, and 1.99. The Reynolds number based on inlet diameter varied from 2.0 to  $2.4 \times 10^6$ .

#### SYMBOLS

The following symbols are used in this report:

- $C_D$  drag coefficient,  $D/q_0 S_m$   
 $C_f$  friction drag coefficient, based on wetted area  
 $C_L$  lift coefficient,  $L/q_0 S_m$   
 $C_M$  pitching-moment coefficient, about the base of the model,  
 $G/q_0 S_m l$   
 $C_p$  pressure coefficient,  $p-p_0/q_0$   
 $D$  drag  
 $d$  diameter at area of maximum cross section, 8.125 inches  
 $G$  pitching moment about base of model  
 $L$  lift  
 $l$  length of model, 58.66 (in.)  
 $M$  Mach number  
 $m_3/m_0$  mass-flow ratio,  $\frac{\rho_3 U_3 S_3}{\rho_0 U_0 S_c}$   
 $P$  total pressure  
 $p$  static pressure  
 $q$  dynamic pressure,  $\gamma p M^2/2$

2039

Re Reynolds number  
S area  
 $S_c$  inlet capture area defined by cowl lip, 0.1674 (sq ft)  
 $S_m$  maximum cross-sectional area, 0.3601 (sq ft)  
U velocity  
u velocity in boundary layer  
 $v_x$  axial perturbation velocity  
 $x, r, \theta$  cylindrical coordinates  
y distance from model surface  
 $\alpha$  angle of attack  
 $\gamma$  ratio of specific heats, 1.40  
 $\delta$  boundary-layer thickness  
 $\rho$  mass density

## Subscripts:

a additive drag  
f friction  
 $l$  local condition in boundary layer  
p pressure  
 $\delta$  conditions at outer edge of boundary layer  
0 free stream  
1 cowl lip  
2 station at 7.00 inches downstream of cowl lip  
3 combustion-chamber inlet

2059

## APPARATUS AND PROCEDURE

A schematic assembly of the model is shown in figure 1(a). The apparatus is similar to that employed in reference 1 except for the inlet, which is detailed in figure 1(b). The inlet was designed so that the oblique shock would intersect the cowl lip at a Mach number of 1.80. The cowl lip had a relatively sharp supersonic profile designed to be approximately tangent to the streamlines immediately behind the oblique shock at a Mach number of 1.80.

Two models designated A and B were investigated. Model A had an internal contraction ratio of 1.04. With this contraction, internal choking occurred at Mach number 1.79 due to the growth of boundary layer, which prevented the normal shock from being swallowed. In order to help alleviate this condition, the spike contour of model B was slightly reduced from that of model A, as shown by the model coordinates presented in table I. In addition to the spike-contour modification, the length of the support struts was decreased  $2\frac{1}{4}$  inches. The same cowl was used for both models.

Shown in figure 2 is the longitudinal variation of the ratio of the local annular area (based on an average of surface normals) to the area of the simulated combustion chamber. The aforementioned modification in spike contour and support-strut length can be seen in this figure.

The model instrumentation and the experimental techniques were similar to those described in reference 1. The location of the static-pressure orifices are given in table II. Flow stations are defined in figure 3.

The internal mass-flow rate was computed by using the average total pressure measured at the combustion-chamber inlet and assuming isentropic flow to the minimum geometric area at the tail plug where choking occurred. A correction factor of 0.97 (determined from shock-swallowed operation) was applied to all mass-flow calculations.

Data were obtained for a range of mass flows and at angles of attack from  $0^\circ$  to  $10^\circ$ . Pressure data were obtained at Mach numbers 1.79 and 1.99 using model A. Force and moment characteristics were determined at Mach number 1.79 with model A and at Mach numbers 1.59, 1.79, and 1.99 with model B.

CONFIDENTIAL

## RESULTS AND DISCUSSION

### External-Flow Characteristics

Zero angle of attack. - The variation of total drag coefficient  $C_D$  with mass-flow ratio  $m_3/m_0$  for model B is presented in figure 4 for the three Mach numbers of the investigation. Unless otherwise noted, all external-pressure data are presented for model A and all force data for model B. The drag represents all the forces external to the entering stream tube and the model shell.

With decreasing mass-flow ratio, the drag coefficient increased rapidly at a rate that increased slightly with free-stream Mach number. The increase in drag coefficient at critical mass-flow ratio with decreasing Mach number, shown in figure 5, was in part due to the increased spillage that accompanied a decrease in the Mach number.

External and internal pressure distributions are presented in tabular form in tables III to V. The longitudinal external-pressure distribution for a range of mass-flow ratios at Mach numbers 1.79 and 1.99 is shown in figure 6. Expansion of the flow around the inlet increased with increasing mass spillage. The most pronounced variations of pressures extended only approximately 2 diameters downstream of the lip.

The decrease in pressure coefficient at  $x/d \approx 4.00$  was caused by expansion of the flow as a result of the change in model contour from a conical to a cylindrical section. At  $x/d \approx 1.22$  the decrease was the result of the joint between the cowl and the afterbody, whereas at  $M_0 = 1.99$  the decrease in pressure coefficient for  $x/d \approx 3.25$  resulted from a weak tunnel disturbance. Close agreement with linearized potential theory (valid only for shock-swallowed conditions) is shown for  $m_3/m_0 = 1.0$  at  $M_0 = 1.99$  and for  $m_3/m_0 = 0.940$  at  $M_0 = 1.79$ . The theoretical computations neglected the influence of the bow shock at the cowl lip, inasmuch as the region affected was of extremely limited extent relative to the model length.

The pressure drag coefficient  $C_{D,p}$ , evaluated from an integration of the external pressures at various mass-flow ratios, is presented in figure 7. The reduction of cowl pressures with increasing spillage resulted in an actual thrust force at mass-flow ratios less than approximately 0.70. Comparison of the experimental and theoretical pressure drags shows good agreement at  $M_0 = 1.99$  for  $m_3/m_0 = 1.0$ . Extrapolation to  $m_3/m_0 = 1.0$  for data at  $M_0 = 1.79$  also indicates good agreement with theory.

Typical radial distributions of local Mach number, measured by the boundary-layer rake at station 51.03, are shown in figure 8 for a range of mass-flow ratios at free-stream Mach numbers of 1.79 and 1.99. The Mach numbers were calculated from the Rayleigh equation by assuming adiabatic flow at free-stream total temperature and uniform radial static pressure at the measured surface value. Local Mach numbers greater than free stream were a consequence of surface static pressures at the rake that were slightly less than ambient (fig. 6). As discussed in reference 3, the form of the profiles and their displacement with mass-flow variation is associated with the total-pressure losses due to flow through the bow shock wave. The method of reference 3 was employed to isolate the bow shock losses from the total losses measured at the individual rake tubes. The boundary-layer thicknesses  $\delta$  were consequently determined to extend to the rapid change in slope of the profiles (shown by arrows in fig. 8). For these values of  $\delta$ , the dimensionless velocity profiles are shown in figure 9 to vary according to the 1/7 power law.

Calculation of the decrement of momentum in the boundary layer yielded the friction drag coefficient, which is shown in figure 10 to be essentially independent of mass flow and free-stream Mach number. Good agreement is indicated in figure 11 between the average value of skin friction coefficient of 0.0018 (based on wetted area) and the von Kármán turbulent compressible theory for flat plates (reference 4). Indicated Reynolds numbers are based on free-stream conditions and the length of the external model shell ahead of the rake.

The variation of additive-drag coefficient with mass-flow ratio is shown in figure 12. Additive drag was obtained from a momentum balance (applied to the flow between flow stations 0 and 2), which included the contribution of the measured pressures along the spike and the cowl. The momentum at station 2 was obtained from the corrected mass flow and the measured static pressure. The additive drag increased rapidly with decreasing mass-flow ratio and increased slightly with Mach number at a given mass-flow ratio. The slightly negative values at  $m_3/m_0 = 1.0$  for  $M_0 = 1.99$  may be partly ascribed to a neglect of viscous effects. Excellent agreement was obtained with the one-dimensional theory of reference 5.

The sum of the drag components evaluated from the pressure data of model A is compared in figure 13 with the total drag obtained from force measurements of model A and B at  $M_0 = 1.79$  and of model B at  $M_0 = 1.99$ . The friction drag was modified from the value given in figure 10 to account for the model length downstream of the boundary-layer rake. Good agreement is shown for model A at  $M_0 = 1.79$ . At  $M_0 = 1.99$  the measured drag of model B was less than the summarized

component drags of model A. Because model A exhibited greater drag values than did model B at  $M_0 = 1.79$ , however, it is presumed that good agreement would result at  $M_0 = 1.99$  from comparison of the same model. Figure 13 shows that for either model the additive drag was directly responsible for the rapid increase in drag with increasing mass-flow spillage.

Angle of attack. - The variation of total drag coefficient with mass-flow ratio is shown in figure 14 for angles of attack to  $10^\circ$ . The rate of drag increase with increasing mass flow spillage was essentially independent of angle of attack. As discussed in references 1 and 2, the increase in drag at a given mass-flow ratio resulted from the increase in normal force while the axial force remained relatively constant.

The lift and-pitching moment coefficients (which include the additive components due to mass spillage) are presented as a function of mass-flow ratio for various angles of attack in figures 15 and 16, respectively. For the determination of the pitching moment, the force on the model due to the inlet flow deflection was assumed to act at the cowl lip. The lift and pitching-moment coefficients decreased slightly with decreasing mass-flow ratio. At a given mass-flow ratio and angle of attack, the lift coefficient increased slightly with free-stream Mach number but the moment coefficient remained approximately constant. The location of the center of pressure (fig. 17) varied between approximately 4.25 and 5.25 diameters ahead of the base.

At critical mass-flow ratios, the drag, drag increment, lift, and pitching moment varied with angle of attack as shown in figure 18. As in references 1 and 2, the modified theory of reference 6 is in good agreement for the moment coefficient at low angles of attack but underestimates the drag increments and lift coefficients.

The effect of angle of attack on the longitudinal pressure distribution is illustrated in figure 19 for Mach number 1.79. Additional data are presented in tables III to V. The decrease in upper-surface pressures with increasing angle of attack extended approximately 2 diameters downstream of the cowl lip. The simultaneous increase in lower-surface pressures extended the length of the model.

#### Internal-Flow Characteristics

Zero angle of attack. - The variation of total-pressure recovery  $P_3/P_0$  and combustion-chamber Mach number  $M_3$  with mass-flow ratio is shown in figure 20. The total pressure  $P_3$  is presented as the corrected value based on the corrected mass flow and the average static

2039

pressure at the rake station rather than the slightly greater value indicated by the combustion-chamber survey rake. Combustion-chamber Mach number  $M_3$  was computed assuming isentropic expansion from the annular area at flow station 3 to the area of the combustion chamber with the sting removed. At Mach number 1.59 the subcritical total-pressure recovery was invariant with mass-flow ratio, whereas at Mach numbers 1.79 and 1.99 the recovery decreased with decreasing mass-flow ratio. Maximum total-pressure recoveries of 90, 87, and 79 percent were obtained at Mach numbers of 1.59, 1.79, and 1.99, respectively.

The components of the over-all total-pressure loss are presented in figure 21 as the inlet losses  $\Delta P_{0-2}/P_0$  and the subsonic-diffuser losses  $\Delta P_{2-3}/P_0$ . The average total pressure  $P_2$  at flow station 2 was computed from the corrected mass flow and local static pressure. Decreasing the mass-flow ratio decreased the losses in the subsonic diffuser but increased the inlet losses.

A comparison of the measured subcritical inlet total-pressure recovery  $P_2/P_0$  and the calculated recovery, the latter determined as in reference 1, is presented in figure 22. The calculated pressure recoveries were approximately 5 percent greater than the measured values. Good agreement can be seen in the slope of the measured and calculated values.

As shown in figure 23, the total-pressure recovery  $P_3/P_2$  of the subsonic diffuser for subcritical mass-flow ratios was relatively independent of Mach number but decreased with increasing mass-flow ratio to approximately 94 percent at critical mass-flow ratios. A large part of this decrease is attributable to the wake effects of the support struts.

Mach number profiles at the combustion-chamber inlet are shown in figure 24 for  $M_0 = 1.79$ . The Mach number variation increased and the peak velocity moved toward the outer shell as the mass-flow ratio increased. The differences in profiles of adjacent rakes was a consequence of the support-strut wake effects.

Angle of attack. - The effect of angle of attack on the subcritical total-pressure recovery and combustion-chamber Mach number was negligible at  $M_0 = 1.59$  (fig. 25). Slight reductions in pressure recovery occurred at an angle of attack of  $10^\circ$  for  $M_0 = 1.79$  and at  $6^\circ$  and  $10^\circ$  for  $M_0 = 1.99$ . Flow instability occurred at  $10^\circ$  for  $M_0 = 1.99$  for mass-flow ratios less than 0.84. Due to the intensity of the instability, no data were taken in this region.

The decrease in maximum mass-flow ratio with angle of attack was greater at an angle of attack of  $10^{\circ}$  than that attributable to the area reduction which occurs when the inlet area is multiplied by the cosine of  $\alpha$ . This mass-flow limitation presumably resulted from premature choking in the upper portion of the subsonic diffuser near the leading edge of the support struts (reference 1).

The inlet and subsonic diffuser components of the over-all total-pressure loss are shown in figure 26 to be essentially independent of angle of attack at  $M_0 = 1.79$ . The minor discrepancy between these data and the pressure recovery at  $10^{\circ}$  angle of attack (fig. 25(b)) is attributable to the slight differences between models A and B.

Increasing the angle of attack to  $10^{\circ}$  resulted in relatively greater total pressure and mass flow in the upper portion of the subsonic diffuser and possible flow separation from the lower diffuser surface. These effects were also noted in references 1 and 2.

#### SUMMARY OF RESULTS

An investigation was conducted at Mach numbers 1.59, 1.79, and 1.99 to determine the force, moment, and pressure characteristics of an all-external compression, conical spike inlet having a supersonic cowl lip. The following results were obtained at an average Reynolds number of 2,300,000 (based on inlet diameter) for a range of mass flows and angles of attack to  $10^{\circ}$ :

1. The rapid increase in drag coefficient with decreasing mass flow and the increase in minimum drag with decreasing Mach number was associated with the increase in additive drag. The drag rise due to angle of attack resulted primarily from an increase in the normal force; the axial force remained relatively constant.
2. The variation of additive drag with mass-flow ratio was satisfactorily calculated from a momentum balance and assuming one-dimensional flow.
3. At zero angle of attack and with no mass spillage, the external pressure distribution and hence the pressure drag were satisfactorily predicted by linearized potential theory.

2039

4. The friction drag was independent of Mach number and mass flow and agreed well with the value predicted by the theory for turbulent compressible flow over a flat plate.

5. The total-pressure recovery was in general only slightly reduced by increases in angle of attack.

Lewis Flight Propulsion Laboratory,  
National Advisory Committee for Aeronautics,  
Cleveland, Ohio.

2629

## REFERENCES

1. Esenwein, Fred T., and Valerino, Alfred S.: Force and Pressure Characteristics for a Series of Nose Inlets at Mach Numbers from 1.59 to 1.99. I - Conical-Spike All-External Compression Inlet with Subsonic Cowl Lip. NACA RM E50J26, 1951.
2. Obery, L. J., and Englert, G. W.: Force and Pressure Characteristics for a Series of Nose Inlets at Mach Numbers from 1.59 to 1.99. II - Isentropic-Spike All-External Compression Inlet. NACA RM E50J26a, 1951.
3. Luidens, Roger W., and Madden, Robert T.: Interpretation of Boundary-Layer Pressure-Rake Data in Flow with a Detached Shock. NACA RM E50I29a, 1950.
4. de Kármán, Th.: The Problem of Resistance in Compressible Fluids. Quinto Convegno "Volta", Reale Accademia d'Italia (Roma), Sett. 30-Ott. 6, 1935, pp. 3-57.
5. Dailey, C. L., and Mc Farland, H. W.: Development of Ramjet Components. Prog. Rep. 9961-8, Univ. Southern Calif. Aero. Lab., USCLA, Feb. 7, 1950. (Bi-Monthly Prog. Rep. Dec. 1949-Jan. 1950 under Navy Contract N)a(s) 9961.)
6. Allen, H. Julian: Estimation of the Forces and Moments Acting on Inclined Bodies of Revolution of High Fineness Ratio. NACA RM A9I26, 1949.

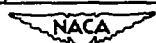
TABLE I - TABLES OF COORDINATES FOR

## 8-INCH RAM-JET CONFIGURATION

(a) Center body coordinates      (b) Outer shell coordinates

Station (in.)	Diameter (in.)	
	Model A	Model B
0.378	2.800	2.800
.500	2.890	2.875
1.000	3.125	3.080
1.500	3.295	3.255
2.000	3.448	3.413
2.500	3.593	3.555
3.000	3.730	3.638
3.500	3.860	3.815
4.000	3.980	3.935
4.500	4.090	4.045
5.000	4.193	4.153
6.000	4.382	4.340
7.000	4.533	4.495
7.750	4.600	4.585
7.910	4.600	4.600
10.000	4.585	4.585
12.000	4.545	4.545
14.000	4.486	4.486
16.000	4.415	4.415
18.000	4.327	4.327
20.000	4.220	4.220
22.000	4.084	4.084
24.000	3.922	3.922
26.000	3.715	3.715
30.030	3.343	3.343

Station	External diameter (in.)	Internal diameter (in.)
0.250	5.660	5.560
.500	5.740	5.615
.750	5.823	5.665
1.000	5.890	5.715
1.500	6.017	5.809
2.000	6.128	5.897
2.500	6.227	5.981
3.000	6.312	6.062
4.000	6.464	6.214
5.000	6.603	6.353
6.000	6.728	6.478
7.000	6.828	6.578
8.000	6.900	6.650
8.375	6.920	6.670
9.905	6.998	6.748
22.000	7.616	7.366
30.000	8.024	7.774
32.000	8.125	7.875
56.000	8.125	7.875



~~CONFIDENTIAL~~

TABLE II - LOCATION OF STATIC-PRESSURE  
ORIFICES FOR PRESSURE MODEL



(a) Location of static tubes (b) Location of static  
along shell contour tubes ( $\theta = 0^\circ$ )

Station		
<sup>a</sup> External	<sup>b</sup> Internal	
0.500	11.000	0.500
1.000	12.000	1.000
1.500	14.000	1.500
2.000	16.000	2.000
2.500	18.000	2.500
3.000	21.000	3.000
4.000	24.000	4.000
5.000	27.000	5.000
6.000	31.000	6.000
7.000	35.000	7.000
8.000	40.000	8.000
9.000	45.000	9.000
10.000		

Station	
Spike	Island
-1.00	8.00
-0.50	9.00
0	10.00
0.50	11.00
1.00	12.00
1.50	14.00
2.00	16.00
2.50	18.00
3.00	21.00
4.00	24.00
5.00	27.00
6.00	31.00
7.00	37.00

<sup>a</sup>Two rows of orifices at  $\theta = 180^\circ$  and  $\theta = 270^\circ$ .

<sup>b</sup> $\theta = 0^\circ$ .

TABLE III - EXTERNAL AND INTERNAL PRESSURE COEFFICIENTS OF NACA 8-INCH RAM-JET CONFIGURATION  
FOR FOUR ANGLES OF ATTACK AT FREE-STREAM MACH NUMBER OF 1.79



Station	$\alpha = 0^\circ; m_3/m_0 = 0.940$				$\alpha = 0^\circ; m_3/m_0 = 0.892$				$\alpha = 0^\circ; m_3/m_0 = 0.765$				$\alpha = 0^\circ; m_3/m_0 = 0.527$				$\alpha = 0^\circ; m_3/m_0 = 0.300$				
	Outer shell		Center body	Outer shell		Center body	Outer shell		Center body	Outer shell		Center body	Outer shell		Center body	Outer shell		Center body			
	External	Internal		External	Internal		External	Internal		External	Internal		External	Internal		External	Internal		External	Internal	
$\theta \rightarrow$	180°	270°	0°	0°	180°	270°	0°	0°	180°	270°	0°	0°	180°	270°	0°	0°	180°	270°	0°	0°	
-1.0				0.504			0.500			0.596			1.287							1.364	
-0.5				.512			.548			1.280			1.324							1.450	
0				.517			1.169			1.246			1.386							1.412	
0.5	0.219	0.203	1.112	.830	0.128	0.116	1.255	.947	0.001	-0.014	1.383	1.118	-0.199	-0.219	1.540	1.357	-0.298	-0.308	1.629	1.535	
1.0	.169	.153	1.057	.980	.134	.115	1.213	1.134	.066	.083	1.350	1.278	-.067	-.080	1.512	1.469	-.190	-.213	1.611	1.590	
1.5	.151	.120	1.064	1.029	.109	.098	1.216	1.182	.068	.066	1.346	1.382	-.024	-.034	1.510	1.497	-.110	-.116	1.607	1.605	
2.0				.080	1.065	1.059		.074	1.211	1.198	.045	1.345	1.385			1.507	1.506			1.607	
2.5	.067	.078	1.044	1.055	.095	.066	1.208	1.198	.064	.045	1.344	1.337	.012	-.006	1.507	1.508	-.043	-.057	1.606	1.607	
3.0	.065	1.042	1.050		.084	1.208	1.198		.054	1.344	1.337					1.508	1.508			1.606	
3.5	.048	.040	1.036	1.039	.038	.055	1.208	1.208	.022	.019	1.344	1.344	-.006	-.005	1.508	1.512	-.032	-.047	1.606	1.607	
4.0	.036	.025	1.003	1.008	.086	.020	1.195	1.192	.012	.008	1.339	1.339	-.008	-.014	1.507	1.510	-.028	-.044	1.606	1.607	
5.0	.018	.008	.984	.937	.010	.004	1.183	1.162	-.001	-.006	1.335	1.319	-.018	-.023	1.507	1.508	-.032	-.036	1.605	1.604	
6.0																					
7.0																					
8.0																					
9.0																					
10.0																					
11.0																					
12.0																					
13.0																					
14.0																					
15.0																					
16.0																					
17.0																					
18.0																					
19.0																					
20.0																					
21.0																					
22.0																					
23.0																					
24.0																					
25.0																					
26.0																					
27.0																					
28.0																					
29.0																					
30.0																					
31.0																					
32.0																					
33.0																					
34.0																					
35.0																					
36.0																					
37.0																					
38.0																					
39.0																					
40.0																					
41.0																					
42.0																					
43.0																					

Station	Outer shell, external				Outer shell, external				Outer shell, external				Outer shell, external				Outer shell, external			
	180°	216°	234°	252°	198°	216°	234°	252°	198°	216°	234°	252°	198°	216°	234°	252°	198°	216°	234°	252°
0.5	0.230	0.237	0.230	0.215	0.146	0.149	0.142	0.127	0.014	0.017	0.012	-0.008	-0.183	-0.178	-0.177	-0.209	-0.294	-0.291	-0.291	-0.301
14.0	-.005	-.004	-.008	.005	-.005	-.008	-.006	.002	-.010	-.013	-.010	-.004	-.017	-.015	-.014	-.012	-.018	-.018	-.016	-.014
43.0	-.010	-.010	-.010	-.012	-.011	-.011	-.012	-.012	-.015	-.012	-.013	-.013	-.013	-.013	-.013	-.014	-.013	-.011	-.014	-.014

TABLE III - EXTERNAL AND INTERNAL PRESSURE COEFFICIENTS OF NACA 8-INCH RAM-JET CONFIGURATION  
FOR FOUR ANGLES OF ATTACK AT FREE-STREAM MACH NUMBER OF 1.79 - Continued

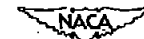


Station	$\alpha = 3^\circ; m_3/m_0 = 0.939$				$\alpha = 3^\circ; m_3/m_0 = 0.893$				$\alpha = 3^\circ; m_3/m_0 = 0.762$				$\alpha = 3^\circ; m_3/m_0 = 0.526$				$\alpha = 3^\circ; m_3/m_0 = 0.303$						
	(a) Continued. Longitudinal distribution of $C_p$ .																						
	Outer shell		Center body	Outer shell		Center body	Outer shell		Center body	Outer shell		Center body	Outer shell		Center body	Outer shell		Center body	Outer shell		Center body		
	External	Internal		External	Internal		External	Internal		External	Internal		External	Internal		External	Internal		External	Internal			
0 →	180°	270°	0°	0°	180°	270°	0°	0°	0°	180°	270°	0°	0°	180°	270°	0°	0°	180°	270°	0°	0°		
-1.0			0.578				0.579			0.676				1.278							1.373		
+0.5			.577				.586			1.222				1.326							1.429		
0			.577				1.140			1.231				1.377							1.492		
0.5	0.098	0.214	0.964	0.477	0.019	0.137	1.162	.842	-0.069	0.004	1.331	1.071	-0.263	-0.194	1.518	1.339	-0.332	-0.329	1.613	1.532			
1.0	.080	.159	.975	.953	.048	.126	1.145	1.075	-.053	.057	1.311	1.245	-.159	-.070	1.491	1.453	-.325	-.265	1.598	1.573			
1.5	.057	.125	1.019	.986	.036	.104	1.168	1.142	-.013	.064	1.322	1.298	-.107	-.029	1.494	1.482	-.257	-.136	1.596	1.588			
2.0		.097	1.019	1.004			.081	1.176	1.163		.061	1.366	1.316		-.016	1.495	1.494		-.100	1.596	1.594		
2.5	.082	.064	1.019	1.010	.032	.072	1.178	1.173	.010	.049	1.331	1.325	-.062	-.003	1.497	1.499	-.184	-.059	1.596	1.596			
3.0		.067	1.024	1.013			.058	1.168	1.178		.037	1.334	1.389		0.003	1.500	1.500		-.058	1.598	1.596		
4.0	-.001	.040	1.086	1.087	-.010	.087	1.191	1.194	-.088	.028	1.340	1.342	-.087	-.008	1.503	1.509	-.095	-.040	1.599	1.599			
5.0	-.006	.027	.998	.996	-.013	.025	1.186	1.185	-.010	.010	1.340	1.340	-.081	-.012	1.506	1.509	-.077	-.058	1.601	1.599			
6.0	-.015	.008	.983	.936	-.025	.004	1.179	1.180	-.033	-.006	1.340	1.325	-.058	-.025	1.507	1.503	-.072	-.043	1.601	1.599			
7.0		-.004	.697	.895			-.008	1.158	1.153		-.016	1.329	1.325		-.050	1.503	1.503		-.045	1.598	1.599		
8.0	-.081	-.007	.922	.893	-.026	-.009	1.176	1.153	-.035	-.018	1.339	1.323	-.045	-.020	1.509	1.503	-.059	-.043	1.602	1.599			
9.0	-.024	-.015	.630	.637	-.026	-.016	1.161	1.155	-.031	-.024	1.332	1.345	-.041	-.024	1.507	1.514	-.053	-.046	1.602	1.504			
10.0		-.027	.021	.801	-.029	-.022	1.186	1.188	-.037	-.027	1.349	1.345	-.048	-.027	1.517	1.517	-.063	-.046	1.604				
11.0	-.030	-.018	.503	-.021	-.020	1.206	1.206	-.028	-.026	1.360	1.360	-.036	-.024	1.521	1.521	-.045	-.044	1.604					
12.0	-.015	-.015	.456	-.016	-.013	1.241	1.241	-.028	-.019	1.381	1.381	-.050	-.026	1.528	1.528	-.056	-.036	1.607					
14.0		-.007	-.008	.289	-.011	-.009	1.311	1.311	-.018	-.015	1.424	1.424	-.018	-.002	1.544	1.544	-.092	-.028	1.612				
16.0	-.009	0	.636	-.011	-.009	1.358	1.358	-.013	-.013	1.469	1.469	-.018	-.019	1.559	1.559	-.022	-.025	1.616					
18.0		.001	-.004	.885	0	-.008	1.408	1.408	-.003	-.018	1.487	1.487	-.007	-.016	1.572	1.572	-.012	-.028	1.620				
21.0	.005	-.005	1.064	.004	-.008	1.463	1.463	.003	-.011	1.528	1.528	-.008	-.015	1.591	1.591	-.006	-.020	1.625					
24.0	.009	-.003	1.183	.006	-.004	1.513	1.513	.005	-.005	1.556	1.556	-.003	-.008	1.607	1.607	-.001	-.012	1.632					
27.0	.002	.001	1.375	-.005	-.001	1.554	0	-.005	1.582	1.582	-.008	-.005	1.619	1.619	-.006	-.008	1.636						
31.0		.004	1.352	-.019		1.580	1.580	-.021		1.595	1.595	-.022		1.626	1.626	-.002	-.025	1.639					
35.0	-.020																						
37.0		-.010	1.375	-.009		1.621	1.621	-.011		1.634	1.634	-.011		1.636	1.636	-.012							
40.0		-.012			-.018			-.012				-.013				-.012							
45.0																							

Station	Outer shell, external				Outer shell, external				Outer shell, external				Outer shell, external				Outer shell, external				
	Outer shell, external				Outer shell, external				Outer shell, external				Outer shell, external				Outer shell, external				
0 →	198°	216°	234°	252°	198°	216°	234°	252°	198°	216°	234°	252°	198°	216°	234°	252°	198°	216°	234°	252°	
0.5	0.180	0.145	0.165	0.186	0.056	0.063	0.084	0.107	-0.081	-0.080	-0.059	-0.025	-0.265	-0.240	-0.227	-0.221	-0.533	-0.532	-0.530	-0.532	
14.0	-.015	-.015	-.010	-.008	-.018	-.018	-.013	-.007	-.019	-.029	-.018	-.011	-.026	-.028	-.023	-.016	-.029	-.033	-.030	-.025	
43.0	-.013	-.013	-.017	-.020	-.013	-.013	-.018	-.021	-.013	-.013	-.018	-.021	-.016	-.015	-.018	-.023	-.017	-.017	-.020	-.023	

TABLE III - EXTERNAL AND INTERNAL PRESSURE COEFFICIENTS OF NACA 8-INCH RAM-JET CONFIGURATION  
FOR FOUR ANGLES OF ATTACK AT FREE-STREAM MACH NUMBER OF 1.78 - Continued



Station	$\alpha = 8^\circ; m_2/m_0 = 0.935$				$\alpha = 6^\circ; m_2/m_0 = 0.698$				$\alpha = 6^\circ; m_2/m_0 = 0.720$				$\alpha = 6^\circ; m_2/m_0 = 0.644$			
	(a) Continued. Longitudinal distribution of $C_p$ .															
	Outer shell		Center body	Outer shell		Center body	Outer shell		Center body	Outer shell		Center body	Outer shell		Center body	
	External	Internal		External	Internal		External	Internal		External	Internal		External	Internal		
$\theta \rightarrow$	180°	270°	0°	180°	270°	0°	0°	180°	270°	0°	0°	0°	180°	270°	0°	0°
-1.0			0.663			0.663				0.791			0.791			1.225
-0.5			.660			.660				1.228			1.228			1.272
0			.682			1.037				1.343			1.343			1.295
0.5	-0.009	0.289	0.784	.326	-0.077	0.157	1.051	.691	-0.229	-0.012	1.315	1.085	-0.297	-0.090	1.390	1.185
1.0	.003	.170	.561	.388	-.058	.141	1.063	1.014	-.132	.048	1.311	1.257	-.192	-.005	1.382	1.383
1.5	-.012	.184	.987	.960	-.038	.116	1.150	1.096	-.108	-.009	1.334	1.315	-.147	.026	1.398	1.380
2.0	.105	1.001	1.008			.092	1.142	1.134		.049	1.344	1.338		.026	1.407	1.400
2.5	-.017	.090	1.006	.993	-.017	.063	1.184	1.152	-.080	.049	1.363	1.350	-.106	.030	1.413	1.410
3.0	.072	1.014	1.002			.068	1.166	1.162		.037	1.361	1.358		.029	1.419	1.416
4.0	-.044	.039	1.017	1.019	-.063	.038	1.176	1.185	-.078	.020	1.370	1.376	-.092	.008	1.429	1.431
5.0	-.041	.021	.993	.990	-.049	.019	1.178	1.180	-.070	-.003	1.376	1.378	-.080	-.005	1.433	1.433
6.0	-.044	.001	.988	.933	-.061	-.002	1.176	1.160	-.067	-.016	1.377	1.367	-.074	-.021	1.436	1.428
7.0	-.015	.896	.894			-.018	1.188	1.155		-.029	1.369	1.387		-.035	1.430	1.429
8.0	-.057	-.062	.911	.883	-.041	-.023	1.177	1.158	-.062	-.034	1.377	1.365	-.056	-.039	1.437	1.428
9.0	-.037	-.053	.845	.881	-.058	-.034	1.165	1.191	-.046	-.044	1.370	1.394	-.060	-.049	1.433	1.442
10.0	-.038	-.041	.781	-.043	-.041		1.195	-.050	-.049		1.388	-.058	-.052		1.433	1.445
11.0	-.022	-.036	.583	-.030	-.041		1.211	-.056	-.049		1.396	-.069	-.064		1.454	
12.0	-.018	-.035	.421	-.020	-.040		1.244	-.027	-.047		1.413	-.027	-.032		1.467	
14.0	-.014	-.034	.275	-.015	-.040		1.308	-.021	-.047		1.446	-.021	-.060		1.492	
16.0	-.007	-.033	.686	-.009	-.036		1.362	-.015	-.044		1.476	-.018	-.047		1.514	
18.0	-.003	-.034	.887	-.001	-.036		1.403	-.004	-.042		1.500	-.006	-.044		1.533	
21.0	.006	-.034	1.057	-.005	-.036		1.454	-.002	-.041		1.584	0	-.042		1.560	
24.0	-.009	-.038	1.180	-.008	-.031		1.500	-.003	-.035		1.563	.008	-.036		1.553	
27.0	.005	-.025	1.268	.003	-.028		1.541	-.002	-.029		1.586	-.002	-.031		1.602	
31.0	.005		1.324	.004			1.568	-.002	-.023		1.595	.002	-.024		1.610	
35.0	-.020			-.022			1.611	-.011			1.620	-.011			1.628	
37.0	.008			1.365	-.008							-.013				
40.0	-.011				-.011							-.013				
(b) Continued. Circumferential distribution of $C_p$ .																
Station	Outer shell, external				Outer shell, external				Outer shell, external				Outer shell, external			
$\theta \rightarrow$	198°	213°	234°	252°	198°	216°	234°	252°	198°	216°	234°	252°	198°	216°	234°	252°
0.5	0.019	0.062	0.107	0.161	-0.062	-0.014	0.040	0.085	-0.193	-0.154	-0.114	-0.074	-0.284	-0.246	-0.192	-0.154
14.0	-.016	-.028	-.055	-.008	-.080	-.030	-.028	-.037	-.026	-.036	-.044	-.046	-.027	-.038	-.046	-.049
43.0	-.017	-.020	-.028	-.038	-.017	-.020	-.028	-.040	-.019	-.023	-.028	-.041	-.019	-.028	-.028	-.041

TABLE III - EXTERNAL AND INTERNAL PRESSURE COEFFICIENTS OF NACA 8-INCH RAM-JET CONFIGURATION  
FOR FOUR ANGLES OF ATTACK AT FREE-STREAM-MACH NUMBER OF 1.79 - Concluded



Station	$\alpha = 6^\circ; m_3/m_0 = 0.302$				$\alpha = 10^\circ; m_3/m_0 = 0.915$				$\alpha = 10^\circ; m_3/m_0 = 0.893$				$\alpha = 10^\circ; m_3/m_0 = 0.722$			
	(a) Concluded. Longitudinal distribution of $C_p$ .															
	Outer shell		Center body	Outer shell		Center body	Outer shell		Center body	Outer shell		Center body	Outer shell		Center body	
	External	Internal		External	Internal		External	Internal		External	Internal		External	Internal		
$\theta \rightarrow$	180°	270°	0°	0°	180°	270°	0°	0°	180°	270°	0°	0°	180°	270°	0°	
-1.0				1.387			0.777			0.777			0.947			
-0.5				1.452			.799			.798			1.167			
0				1.485			.798			.830			1.190			
0.5	-0.342	-0.318	1.696	1.515	-0.155	0.241	0.677	.559	-0.204	0.181	1.227	.568	-0.260	0.025	1.198	.998
1.0	-.389	-.189	1.698	1.582	-.108	.184	.516	.267	-.174	.171	.986	.958	-.214	.068	1.228	1.188
1.5	-.306	-.113	1.588	1.580	-.108	.146	.582	.148	-.138	.141	1.087	1.052	-.189	.068	1.273	1.253
2.0	-.080	1.588	1.588	1.588			.864	.409		.108	1.106	1.095		.076	1.292	1.288
2.5	-.174	-.052	1.590	1.580	-.091	.095	.850	.880	-.102	.093	1.129	1.184	-.149	.065	1.309	1.310
3.0	-.043	1.593	1.591	1.593	-.072	.960	.945	.070	1.151	1.143			.047	1.325	1.324	
4.0	-.142	-.088	1.588	1.598	-.084	.031	.979	.976	-.110	.054	1.172	1.175	-.136	.021	1.341	1.349
5.0	-.116	-.034	1.598	1.595	-.074	.010	.962	.958	-.091	.010	1.180	1.177	-.114	-.004	1.353	1.354
6.0	-.103	-.044	1.600	1.598	-.084	-.018	.950	.908	-.074	.019	1.183	1.164	-.083	-.029	1.358	1.349
7.0	-.062	1.598	1.598	1.598			-.056	.875	.871	-.058	1.177	1.169		.048	1.353	1.353
8.0	-.070	-.054	1.601	1.600	-.045	-.048	.875	.848	-.051	-.048	1.199	1.178	-.067	-.067	1.364	1.363
9.0	-.069	-.082	1.601	1.605	-.044	-.064	.799	.832	-.048	-.065	1.203	1.218	-.060	-.072	1.356	1.373
10.0	-.068	-.065	1.604	1.604	-.040	-.069		.723	-.043	-.074		1.229	1.229	-.048	-.081	1.377
11.0	-.043		1.604	1.604	-.025	-.078		.525	-.050	-.079		1.245	1.245	-.034	-.086	1.387
12.0	-.051	-.064		1.608	-.080	-.080		.372	-.026	-.088		1.273	1.273	-.027	-.095	1.403
14.0	-.096	-.060		1.611	-.009	-.096		.234	-.014	-.096		1.327	1.327	-.017	-.101	1.438
16.0	-.016	-.087		1.618	-.004	-.096		.778	-.006	-.104		1.371	1.371	-.008	-.111	1.470
18.0	-.007	-.080		1.619	.006	-.102		.924	.004	-.112		1.406	1.406	.001	-.118	1.495
21.0	-.003	-.046		1.624	.011	-.107		1.058	.006	-.117		1.453	1.453	.006	-.184	1.526
24.0	0	-.037		1.629	.014	-.097		1.141	.012	-.108		1.495	1.495	.009	-.111	1.559
27.0	-.004	-.080		1.632	.011	-.086		1.230	.006	-.094		1.553	1.553	-.006	-.095	1.582
31.0	0			1.635	.012			1.272	.011			1.561	1.561	.009		1.585
35.0	-.026			1.637	-.020			1.318	-.023			1.600	1.600	-.026		1.617
37.0	-.011				-.005				-.004				-.006			
40.0	-.013				-.012				-.012				-.013			
(b) Concluded. Circumferential distribution of $C_p$ .																
Station	Outer shell, external				Outer shell, external				Outer shell, external				Outer shell, external			
$\theta \rightarrow$	198°	216°	234°	252°	198°	216°	234°	252°	198°	216°	234°	252°	198°	216°	234°	252°
0.5	-0.342	-0.337	-0.329	-0.325	-0.104	-0.045	0.037	0.139	-0.176	-0.126	-0.061	-0.048	-0.251	-0.209	-0.157	-0.064
14.0	-.051	-.042	-.058	-.058	-.092	-.045	-.079	-.104	-.026	-.050	-.086	-.117	-.029	-.053	-.090	-.124
43.0	-.019	-.023	-.028	-.041	-.033	-.042	-.045	-.062	-.033	-.045	-.046	-.064	-.033	-.046	-.047	-.064

TABLE IV - EXTERNAL AND INTERNAL PRESSURE COEFFICIENTS OF NACA 8-INCH RAM-JET CONFIGURATION  
FOR FOUR ANGLES OF ATTACK AT FREE-STREAM MACH NUMBER OF 1.79 WITH MODEL ROTATED 180°



Station	$\alpha = 0^\circ; m_3/m_0 = 0.940$			$\alpha = 0^\circ; m_3/m_0 = 0.885$			$\alpha = 0^\circ; m_3/m_0 = 0.754$			$\alpha = 0^\circ; m_3/m_0 = 0.519$		
	(a) Longitudinal distribution of $C_p$ .											
	Outer shell		Center body	Outer shell		Center body	Outer shell		Center body	Outer shell		Center body
	External	Internal		External	Internal		External	Internal		External	Internal	
$\theta \rightarrow$	0°	90°	180°	180°	0°	90°	180°	0°	90°	180°	0°	90°
-1.0			0.503			0.504			0.605			1.276
-0.5			.504			.585			1.234			1.333
0			.522			1.187			1.258			1.397
0.5	0.215	0.217	1.066	.898	0.116	0.118	1.218	.970	-0.006	-0.008	1.134	-0.243
1.0	.162	.163	1.066	.999	.118	.121	1.153	.052	.057	1.544	1.291	-.089
1.5	.118	.129			.090	.101		.050	.061			-.046
2.0	.095	.100	1.066	1.036	.073	.079	1.228	1.203	.044	.051	1.357	-.028
2.5	.081	.088		1.048	.064	.071		1.219	.043	.049	1.351	-.012
3.0	.071			1.046		.058		1.219		.038	1.362	-.004
4.0	.057	.045	1.054	1.055	.028	.037	1.224	1.227	.012	.021	1.352	-.017
5.0	.025	.051		1.023	.020	.025		1.216	.005	.012	1.352	-.017
6.0	.013	.015	.987	.959	.006	.009	1.205	1.185	-.004	-.002	1.348	-.022
7.0		.003		.919		-.001		1.175		-.010	1.331	-.023
8.0	.004	.004		.912	-.001	.002		1.167	-.010	-.007	1.324	-.022
9.0	0			.922		.004		1.187		-.004	1.344	-.018
10.0	.001	0		.847	.004	.002		1.180	.003	-.005	1.344	-.012
11.0	.003	-.003		.909	.001	-.004		1.198	-.008	-.011	1.365	-.015
12.0	.004	.008		1.010	-.004	.012		1.237	-.002	.007	1.375	-.010
14.0	-.004	.007		1.069	-.006	.004		1.309	-.010	0	1.419	-.015
16.0	-.012	-.005		1.244	-.014	-.010		1.367	-.020	-.015	1.456	-.025
18.0	.014	-.007		1.315	.007	-.009		1.412	-.003	-.012	1.486	0
21.0	.017	.007		1.408	.012	.002		1.474	.006	.003	1.525	.004
24.0	.014	.001		1.484	.009	-.002		1.525	.006	.005	1.558	.005
27.0	.004	.006		1.536	.009	.002		1.565	-.002	0	1.586	-.004
31.0	.004			1.574	.002			1.591	0		1.599	-.002
35.0	-.020				-.019				-.020			-.021
37.0				1.615				1.627			1.626	
40.0	-.007				.007				-.010			-.008
45.0	-.011				-.010				-.012			-.012

Station	Outer shell, external				Outer shell, external				Outer shell, external				Outer shell, external			
	Outer shell, external				Outer shell, external				Outer shell, external				Outer shell, external			
	0 →	18°	36°	54°	72°	18°	36°	54°	72°	18°	36°	54°	72°	18°	36°	54°
0.5	0.226	0.254	0.235	0.226	0.124	0.133	0.134	0.124	0	0.008	0.012	0.001	-0.240	-0.227	-0.217	-0.244
14.0	-.004	-.007	-.006	.005	-.009	-.013	-.011	-.006	-.015	-.020	-.014	0	-.021	-.025	-.021	-.006
45.0	-.008	-.008	-.010	-.012	-.010	-.009	-.012	-.012	-.011	-.011	-.012	-.013	-.011	-.010	-.012	-.013

TABLE IV - EXTERNAL AND INTERNAL PRESSURE COEFFICIENTS  
FOR FOUR ANGLES OF ATTACK AT FREE-STREAM MACH NUMBER OF

CA 8-INCH RAM-JET CONFIGURATION  
1TH MODEL ROTATED 180° - Continued

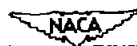


Station	$\alpha = 0^\circ; m_3/m_0 = 0.285$			$\alpha = 3^\circ; m_3/m_0 = 0.940$			$\alpha = 3^\circ; m_3/m_0 = 0.893$			$\alpha = 3^\circ; m_3/m_0 = 0.754$			
	(a) Continued. Longitudinal distribution of $C_p$ .												
	Outer shell		Center body	Outer shell		Center body	Outer shell		Center body	Outer shell		Center body	
	External	Internal		External	Internal		External	Internal		External	Internal		
0 →	0°	90°	180°	180°	0°	90°	180°	180°	0°	90°	180°	180°	
-1.0				1.868			0.432			0.432			0.526
-0.5				1.454			.431			.506			1.168
0				1.503			.527			1.152			1.258
0.5	-0.338	-0.333	1.606	1.558	0.325	0.201	1.163	1.087	0.277	-0.138	1.031	0.139	1.178
1.0	-.248	-.248		1.597	.252	.168			.230	.151	1.238	.167	1.365
1.5	-.140	-.129			.197	.124			.161	.107		.147	1.313
2.0	-.099	-.094	1.605	1.602	.185	.098	1.131	1.101	.153	.083	1.231	.128	1.362
2.5	-.071	-.064		1.605	.146	.084			.155	.073		.1215	1.358
3.0	-.051			1.605		.068				.059		.1210	.041
4.0	-.048	-.038	1.605	1.606	.087	.042	1.100	1.098	.080	.038	1.205	.1210	1.356
5.0	-.039	-.030		1.605	.072	.027			.071	.054		.1191	.035
6.0	-.039	-.028	1.603	1.602	.051	.010	1.043	1.017	.046	.008	1.172	.1562	1.345
7.0	-.036			1.602		.001				.004		.131	1.325
8.0	-.035	-.028		1.602	.053	-.003			.082			.106	1.312
9.0	-.023			1.602		.007			.068	.031		.111	1.298
10.0	-.023	-.023		1.602	.038	-.007			.080	.053		.096	1.309
11.0	-.025	-.025		1.803	.021	-.010			.083	.018		.106	1.306
12.0	-.018	-.007		1.604	.059	.005			.082	.036		.155	1.313
14.0	-.002	-.012		1.610	.028	.005			.170	.020		.250	1.357
16.0	-.030	-.024		1.615	.008	-.015			.263	.006		.325	1.388
18.0	-.006	-.016		1.619	.008	-.018			.354	.006		.379	1.451
21.0	0	-.010		1.626	.023	-.005			.426	.021		.455	1.466
24.0	-.002	-.010		1.630	.021	-.010			.502	.020		.516	1.513
27.0	-.007	-.004		1.635	.008	-.007			.551	.006		.558	1.553
31.0	-.003			1.638	.010				.586	.008		.583	1.583
35.0	-.023				-.016					-.018			1.598
37.0				1.639					1.638			1.619	1.624
40.0	-.010				-.008					-.006			
45.0	-.013				-.010					-.010			

(b) Continued. Circumferential distribution of  $C_p$ .

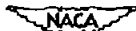
Station	Outer shell, external				Outer shell, external				Outer shell, external				Outer shell, external			
	18°	36°	54°	72°	18°	36°	54°	72°	18°	36°	54°	72°	18°	36°	54°	72°
0.5	-0.334	-0.354	-0.332	-0.334	0.329	0.321	0.296	0.252	0.278	0.269	0.240	0.189	0.141	0.132	0.109	0.054
14.0	-.027	-.030	-.026	-.012	-.016	.008	.003	.018	.013	.005	.001	.010	.007	-.002	-.007	-.004
43.0	-.012	-.012	-.013	-.015	-.007	-.010	-.015	-.020	-.008	-.010	-.015	-.020	-.009	-.011	-.015	-.020

TABLE IV - EXTERNAL AND INTERNAL PRESSURE COEFFICIENTS OF NACA 8-INCH RAM-JET CONFIGURATION  
FOR FOUR ANGLES OF ATTACK AT FREE-STREAM MACH NUMBER OF 1.79 WITH MODEL ROTATED 180° - Continued



Station	$\alpha = 3^\circ; m_3/m_0 = 0.517$				$\alpha = 5^\circ; m_3/m_0 = 0.291$				$\alpha = 6^\circ; m_3/m_0 = 0.940$				$\alpha = 6^\circ; m_3/m_0 = 0.886$			
	(a) Continued. Longitudinal distribution of $C_p$ .															
	Outer shell		Center body	Outer shell		Center body	Outer shell		Center body	Outer shell		Center body	Outer shell		Center body	
	External	Internal		External	Internal		External	Internal		External	Internal		External	Internal		
$\bullet \rightarrow$	0°	90°	180°	180°	0°	90°	180°	180°	0°	90°	180°	180°	0°	90°	180°	180°
-1.0				1.263			1.555			0.364			0.363			0.363
-0.5				1.329			1.427			.363			.363			.429
0				1.401			1.505			.448			.448			1.160
0.5	-0.086	-0.230		1.391	-0.307	-0.336	1.545	0.448	0.226	1.026	0.420	0.181	1.120			1.120
1.0	.023	-0.083	1.525	1.491	-.125	-.261	1.616	1.595	.345	.174	1.196	1.117	.329	.132	1.307	1.238
1.5	.049	-0.032			-.055	-.132			.278	.139			.267	.111		
2.0	.059	-.018	1.525	1.517	-.018	-.094	1.611	1.608	.237	.108	1.124	1.090	.229	.088	1.277	1.254
2.5	.064	-.003			1.523	.004	-.064		1.608	.214			1.092	.209	.080	1.254
3.0				1.522			1.602			.076			1.076			1.242
4.0	.058	-.007	1.517	1.522	.009	-.038	1.606	1.608	.140	.046	1.068	1.069	.156	.034	1.232	1.234
5.0	.031	-.010			1.517	.009	-.032		1.501	.118			1.028	.114	.018	1.210
6.0	.016	-.020	1.512	1.507	-.038	1.608	1.601	.094	.007	.988			.960	.090	0	1.187
7.0		-.026		1.503		-.040			.599				.908		-.015	1.137
8.0	.008	-.023			1.497	-.004	-.033		1.598	.068			.914	.063	-.017	1.097
9.0		-.018			1.502		-.030		1.598				.926		-.019	1.073
10.0	.010	-.021			1.500	0	-.031		1.596	.071			.824	.067	-.024	1.017
11.0	-.003	-.024			1.504	-.010	-.031		1.598	.081			.629	.047	-.027	1.038
12.0	.008	-.010			1.613	.009	-.018		1.601	.080			.457	.069	-.025	1.104
14.0	.005	-.015			1.533	-.002	-.020		1.607	.059			1.049	.065	-.030	1.217
16.0	-.007	-.028			1.551	-.012	-.033		1.615	.038			1.175	.022	-.047	1.300
18.0	0	-.023			1.567	-.003	-.024		1.618	.026			1.283	.024	-.048	1.365
21.0	.010	-.013			1.588	.008	-.018		1.624	.041			1.374	.037	-.055	1.447
24.0	.010	-.015			1.607	.008	-.018		1.631	.038			1.462	.035	-.038	1.512
27.0	.001	-.010			1.621	-.002	-.013		1.635	.025			1.617	.022	-.037	1.552
31.0	.004				1.628	.003			1.638	.034			1.558	.020		1.577
35.0	-.018					-.026				-.003				-.005		
37.0									1.641				1.594			1.615
40.0	-.007					-.008				.005				.004		
45.0	-.010					-.012				.002				-.002		
	(b) Continued. Circumferential distribution of $C_p$ .															
Station	Outer shell, external				Outer shell, external				Outer shell, external				Outer shell, external			
$\bullet \rightarrow$	18°	36°	54°	72°	18°	36°	54°	72°	18°	36°	54°	72°	18°	36°	54°	72°
0.5	-0.086	-0.091	-0.114	-0.168	-0.311	-0.312	-0.315	-0.332	0.445	0.424	0.379	0.310	0.418	0.389	0.324	0.230
14.0	-.002	-.010	-.015	-.005	-.007	-.017	-.020	-.010	.049	.028	.009	.003	.046	.024	.003	
45.0	-.010	-.012	-.016	-.021	-.010	-.012	-.018	-.021	.002	-.010	-.024	-.040	-.002	-.012	-.028	-.043

TABLE IV - EXTERNAL AND INTERNAL PRESSURE COEFFICIENTS OF NACA 8-INCH RAM-JET CONFIGURATION  
FOR FOUR ANGLES OF ATTACK AT FREE-STREAM MACH NUMBER OF 1.79 WITH MODEL ROTATED 180° - Concluded



Station	$\alpha = 6^\circ; m_3/m_0 = 0.762$				$\alpha = 6^\circ; m_3/m_0 = 0.818$				$\alpha = 10^\circ; m_3/m_0 = 0.930$				$\alpha = 10^\circ; m_3/m_0 = 0.885$			
	(a) Concluded. Longitudinal distribution of $C_p$ .															
	Outer shell		Center body	Outer shell		Center body	Outer shell		Center body	Outer shell		Center body	Outer shell		Center body	
	External	Internal		External	Internal		External	Internal		External	Internal		External	Internal		
0 →	0°	90°	180°	180°	0°	90°	180°	180°	0°	90°	180°	180°	0°	90°	180°	180°
-1.0				0.435			1.245			0.308			0.764			
-0.5				1.128			1.324			.308			.768			
0				1.280			1.406			.739			.813			
0.5	0.300	0.008	1.407	1.221	0.049	-0.189	1.406	0.591	0.244	1.085	0.593	0.168	.929			
1.0	.384	.071		1.341	.140	-.070	1.536	1.506	.450	.195	1.164	.455	.182	1.201	1.114	
1.5	.241	.077			.150	-.025			.368	.156		.375	.149			
2.0	.212	.059	1.588	1.370	.145	-.012	1.534	1.589	.318	.120	1.107	1.093	.324	.110	1.252	1.294
2.5	.194	.058		1.372	.141	-.004		1.531	.288	.101		1.078	.294	.097	1.286	
3.0		.044		1.365		.001		1.528		.080		1.068		.074	1.266	
4.0	.127	.021	1.357	1.360	.095	-.005	1.620	1.525	.205	.047	1.048	1.048	.212	.043	1.220	1.233
5.0	.106	.008		1.344	.079	-.014		1.517	.178	.026		1.013	.186	.031	1.198	
6.0	.083	-.010	1.329	1.314	.060	-.025	1.509	1.504	.148	.001	.978	.951	.156	-.007	1.161	1.146
7.0		-.022		1.296		.037		1.496		.023		.906		-.030	1.104	
8.0	.058	-.028		1.267	.041	-.037		1.488	.118	-.036		.904	.124	-.041	1.059	
9.0		-.025		1.267		.036		1.489		.048		.906		-.053	1.016	
10.0	.059	-.030		1.249	.044	-.037		1.484	.112	-.061		.797	.117	-.066	.950	
11.0	.041	-.032		1.260	.086	-.044		1.497	.094	-.074		.601	.098	-.078	.964	
12.0	.052	-.031		1.287	.041	-.043		1.494	.102	-.081		.429	.106	-.083	1.039	
14.0	.049	-.034		1.562	.026	-.045		1.619	.100	-.085		.956	.101	-.083	1.166	
16.0	.031	-.061		1.402	.021	-.057		1.539	.081	-.096		1.100	.083	-.099	1.256	
18.0	.018	-.048		1.445	.010	-.048		1.687	.069	-.105		1.195	.074	-.102	1.323	
21.0	.036	-.037		1.503	.026	-.040		1.581	.075	-.101		1.309	.076	-.103	1.412	
24.0	.058	-.038		1.548	.024	-.040		1.601	.070	-.104		1.395	.072	-.105	1.480	
27.0	.081	-.038		1.578	.014	-.037		1.615	.067	-.101		1.446	.060	-.100	1.523	
31.0	.020			1.591	.016			1.621	.053			1.481	.067		1.549	
35.0	-.007				-.010					.022			.028			
37.0				1.618				1.632				1.613			1.584	
40.0	.005				.001				.030				.035			
45.0	-.002				-.003				.023				.029			

(b) Concluded. Circumferential distribution of  $C_p$ .

Station	Outer shell, external				Outer shell, external				Outer shell, external				Outer shell, external			
	18°	36°	54°	72°	18°	36°	54°	72°	18°	36°	54°	72°	18°	36°	54°	72°
0.5	0.292	0.257	0.194	0.103	0.034	0.009	-0.037	-0.113	0.586	0.541	0.468	0.368	0.590	0.548	0.472	0.346
14.0	.058	.019	-.001	-.010	.027	.009	-.010	-.021	.086	.066	.007	-.035	.086	.058	.004	-.040
43.0	-.002	-.012	-.027	-.043	-.003	-.014	-.028	-.043	.018	-.014	-.052	-.089	.028	-.010	-.049	-.087



TABLE V - EXTERNAL AND INTERNAL PRESSURE COEFFICIENTS OF NACA 2-INCH RAM-JET CONFIGURATION  
FOR FOUR ANGLES OF ATTACK AT FREE-STREAM MACH NUMBER OF 1.99

CONFIDENTIAL

NACA RM E50J30

Station	$\alpha = 0^\circ; m_3/m_0 = 1.00$				$\alpha = 0^\circ; m_3/m_0 = 0.901$				$\alpha = 0^\circ; m_3/m_0 = 0.738$				$\alpha = 0^\circ; m_3/m_0 = 0.445$				$\alpha = 0^\circ; m_3/m_0 = 0.287$			
	Outer shell		Center body	Outer shell		Center body	Outer shell		Center body	Outer shell		Center body	Outer shell		Center body	Outer shell		Center body		
	External	Internal		External	Internal		External	Internal		External	Internal		External	Internal		External	Internal			
0 →	180°	270°	0°	0°	180°	270°	0°	0°	0°	180°	270°	0°	0°	180°	270°	0°	0°	180°	270°	0°
-1.0			0.477				0.475			0.587				1.401						1.423
-0.8			.477				.492			1.240				1.441						1.492
0			.477				1.125			1.400				1.504						1.562
0.5	0.210	0.204	0.639	.215	0.157	0.157	1.309	1.075	0.005	0.003	1.498	1.238	-0.200	-0.208	1.638	1.476	0.248	-0.244	1.675	1.575
1.0	.157	.151	.707	.143	.135	.130	1.291	1.247	.064	.060	1.473	1.411	-.078	-.075	1.616	1.589	-.154	-.161	1.662	1.545
1.5	.123	.121	.503	.402	.106	.104	1.288	1.300	.066	.063	1.473	1.454	-.088	-.028	1.614	1.610	-.076	-.074	1.659	1.659
2.0	.101	.098	.506	.606	.087	.081	1.277	1.316	.059	.052	1.473	1.468	-.004	-.014	1.615	1.620	-.040	-.050	1.660	1.664
2.5	.089	.086	.456	.554	.077	.071	1.286	1.319	.062	.049	1.473	1.478	.005	0	1.615	1.621	-.086	-.028	1.650	1.665
3.0	.072	.070	.582	.592	.061	.067	1.501	1.518	.037	.058	1.475	1.473	.001	0	1.617	1.621	-.082	-.028	1.682	1.664
4.0	.047	.047	.415	.892	.037	.041	1.235	1.331	.022	.024	1.476	1.483	-.005	0	1.620	1.626	-.018	-.013	1.663	1.657
5.0	.036	.033	.551	.436	.027	.025	1.308	1.320	.012	.012	1.476	1.478	-.005	0	1.622	1.628	-.016	-.018	1.684	1.667
6.0	.022	.018	.491	.540	.014	.012	1.502	1.297	.001	0	1.475	1.465	-.016	-.017	1.624	1.622	-.022	-.023	1.665	1.655
7.0	.007	.007	.537	.465	-.002	.002	1.288	1.290	-.013	-.009	1.475	1.466	-.027	-.025	1.622	1.622	-.002	-.028	1.684	1.654
8.0	.007	.005	.596	.399	0	.001	1.285	1.279	-.010	-.009	1.473	1.458	-.022	-.022	1.624	1.621	-.027	-.027	1.665	1.654
9.0	0	-.005	.448	.494	-.004	-.008	1.276	1.503	-.012	-.017	1.466	1.478	-.023	-.028	1.622	1.627	-.027	-.032	1.665	1.658
10.0	-.012	-.010	.790	-.021	-.010	1.301	-.029	-.019	1.480	-.038	-.029	1.629	-.042	-.033	1.659					
11.0	0	-.008	.579	-.007	-.012	1.315	-.014	-.019	1.488	-.064	-.039	1.632	-.027	-.032	1.669					
12.0	-.005	-.003	.475	-.002	-.005	1.346	-.010	-.012	1.506	-.019	-.021	1.637	-.022	-.024	1.672					
14.0	.005	-.001	.997	0	-.002	1.410	-.008	-.009	1.541	-.014	-.016	1.650	-.018	-.018	1.677					
15.0	.006	-.004	1.129	0	-.002	1.463	-.007	-.008	1.578	-.013	-.016	1.651	-.016	-.018	1.683					
18.0	-.010	-.004	1.234	-.006	-.001	1.508	-.001	-.005	1.598	-.005	-.012	1.672	-.008	-.009	1.687					
21.0	.015	-.005	1.341	-.011	-.003	1.566	-.006	-.008	1.636	-.001	-.007	1.697	-.008	-.009	1.694					
24.0	.026	-.017	1.435	-.020	-.014	1.620	-.014	-.010	1.675	-.008	-.006	1.701	-.006	-.008	1.701					
27.0	-.002	-.007	1.504	-.007	-.003	1.661	-.010	0	1.700	-.016	-.006	1.709	-.017	-.007	1.706					
31.0	0	1.550	-.001	1.685	0	-.021	1.714	-.008	1.731	-.014	1.720	-.004	1.716	-.004	1.707					
35.0	-.017	1.598	-.018	1.718	-.012	-.009	1.731	-.012	1.731	-.012	1.730	-.004	1.724	-.004	1.709					
40.0	-.010	1.598	-.018	1.718	-.008	1.731	-.009	1.731	-.012	1.731	-.012	1.730	-.016	1.724	-.016	1.709				
45.0	-.006	1.598	-.008	1.718	-.008	1.731	-.009	1.731	-.012	1.731	-.012	1.730	-.012	1.724	-.012	1.709				

(b) Circumferential distribution of  $C_p$ .

Station	Outer shell, external				Outer shell, external				Outer shell, external				Outer shell, external				Outer shell, external			
	198°	216°	234°	252°	198°	216°	234°	252°	198°	216°	234°	252°	198°	216°	234°	252°	198°	216°	234°	252°
0 →	0.218	0.224	0.224	0.213	0.170	0.179	0.177	0.168	0.080	0.028	0.028	0.015	-0.191	-0.183	-0.181	-0.200	-0.241	-0.238	-0.237	-0.242
0.5	0.218	0.224	0.224	0.213	0.170	0.179	0.177	0.168	0.080	0.028	0.028	0.015	-0.191	-0.183	-0.181	-0.200	-0.241	-0.238	-0.237	-0.242
14.0	.004	0	0	.003	-.003	-.005	-.006	0	-.009	-.013	-.012	-.008	-.017	-.019	-.018	-.016	-.019	-.022	-.022	-.018
43.0	-.006	-.005	-.008	-.008	-.009	-.007	-.008	-.010	-.010	-.009	-.010	-.012	-.012	-.013	-.014	-.013	-.012	-.013	-.013	-.014

TABLE V - EXTERNAL AND INTERNAL PRESSURE COEFFICIENTS OF NACA 8-INCH RAM-JET CONFIGURATION  
FOR FOUR ANGLES OF ATTACK AT FREE-STREAM MACH NUMBER OF 1.99 - Continued

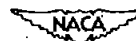


Station	$\alpha = 5^\circ; m_3/m_0 = 0.999$				$\alpha = 5^\circ; m_3/m_0 = 0.909$				$\alpha = 5^\circ; m_3/m_0 = 0.807$				$\alpha = 5^\circ; m_3/m_0 = 0.289$				$\alpha = 5^\circ; m_3/m_0 = 0.995$							
	(a) Continued. Longitudinal distribution of $C_p$ .																							
	Outer shell		Center body	Outer shell		Center body	Outer shell		Center body	Outer shell		Center body	Outer shell		Center body	Outer shell		Center body	Outer shell		Center body			
	External	Internal		External	Internal		External	Internal		External	Internal		External	Internal		External	Internal		External	Internal				
$\theta \rightarrow$	180°	270°	0°	0°	180°	270°	0°	0°	0°	180°	270°	0°	0°	180°	270°	0°	0°	180°	270°	0°	0°			
-1.0			0.556				0.554			1.314			1.437								0.640			
-0.5			.556				.553			1.408			1.485								.639			
0			.557				.598			1.428			1.551								.640			
0.5	0.153	0.208	0.529	.280	0.048	0.160	1.264	.980	-.0162	-0.074	1.545	1.332	-0.245	-0.220	1.670	1.577	0.061	0.210	0.384	.359				
1.0	.090	.154	.587	.400	.056	.135	1.261	1.805	-.078	.006	1.589	1.487	-.214	-.149	1.658	1.641	.087	.154	.541	.526				
1.5	.063	.123	.457	.344	.041	.105	1.276	1.865	-.046	.028	1.584	1.584	-.166	-.069	1.658	1.655	.006	.125	.409	.388				
2.0	.048	.098	.305	.074	.031	.083	1.288	1.290	-.029	.028	1.537	1.537	-.102	-.047	1.660	1.661	-.008	.087	.358	.033				
2.5	.038	.067	.390	.475	.061	.073	1.294	1.304	-.026	.033	1.541	1.545	-.084	-.025	1.663	1.663	-.009	.085	.324	.340				
3.0	.025	.070	.254	.358	.007	.069	1.307	1.307	-.029	.024	1.548	1.548	-.075	-.020	1.665	1.665	-.019	.069	.195	.311				
4.0	.008	.048	.572	.292	-.007	.041	1.313	1.326	-.033	.017	1.551	1.558	-.062	-.003	1.667	1.667	-.035	.042	.284	.260				
5.0	.008	.033	.361	.435	-.010	.068	1.316	1.381	-.031	.004	1.557	1.561	-.052	-.015	1.668	1.670	-.031	.026	.344	.333				
6.0	-.010	.016	.542	.377	-.081	.018	1.314	1.300	-.040	-.010	1.561	1.558	-.055	-.006	1.671	1.670	-.056	.006	.775	.716				
7.0	-.020	.004	.615	.578	-.051	0	1.300	1.298	-.046	-.019	1.561	1.561	-.057	-.051	1.672	1.671	-.041	-.007	.734	.706				
8.0	-.017	0	.760	.746	-.085	-.002	1.511	1.293	-.058	-.018	1.569	1.561	-.048	-.089	1.675	1.674	-.034	-.014	.834	.813				
9.0	-.019	-.007	.790	.804	-.024	-.012	1.802	1.323	-.056	-.026	1.570	1.577	-.044	-.056	1.677	1.677	-.051	-.025	.799	.829				
10.0	-.026	-.018	.804	.804	-.038	-.014		1.325	-.049	-.026	1.885	1.885	-.055	-.035	1.679	1.679	-.058	-.028		.796				
11.0	-.013	-.013	.524	-.021	-.017		1.340	-.031	-.029	1.587	1.587	-.056	-.058	1.680	1.680	-.020	-.029		.610					
12.0	-.008	-.011	.484	-.016	-.018		1.368	-.025	-.025	1.698	1.698	-.030	-.035	1.681	1.681	-.014	-.031		.558					
14.0	-.005	-.010	.996	-.010	-.018		1.426	-.019	-.021	1.613	1.613	-.023	-.029	1.685	1.685	-.006	-.053		1.016					
16.0	-.001	-.005	1.181	-.007	-.010		1.470	-.014	-.020	1.629	1.629	-.018	-.026	1.689	1.689	-.002	-.035		1.128					
18.0	.008	-.002	1.209	-.008	-.007		1.507	-.004	-.016	1.643	1.643	-.007	-.021	1.691	1.691	-.009	-.035		1.207					
21.0	.014	-.002	1.380	.014	-.007		1.581	.010	-.012	1.685	1.685	-.009	-.016	1.695	1.695	-.024	-.034		1.307					
24.0	.014	.008	1.411	.007	.005		1.610	.001	-.002	1.685	1.685	-.002	-.004	1.699	1.699	-.007	-.026		1.393					
27.0	-.008	0	1.480	-.012	-.002		1.650	-.018	-.009	1.701	1.701	-.020	-.018	1.704	1.704	-.010	-.026		1.460					
31.0	.004		1.589	-.002			1.676	-.008		1.711	1.711	-.004		1.704	1.704	-.004			1.508					
35.0	-.018			-.020				-.024		1.721	1.721	-.026		1.706	1.706	-.021			1.553					
37.0							1.711	-.012							1.706	-.006								
40.0	-.008				-.009			-.009								-.005								
45.0	-.005				-.007			-.009																

Station	Outer shell, external								Outer shell, external								Outer shell, external							
	Outer shell, external				Outer shell, external				Outer shell, external				Outer shell, external				Outer shell, external				Outer shell, external			
$\theta \rightarrow$	198°	216°	234°	252°	198°	216°	234°	252°	198°	216°	234°	252°	198°	216°	234°	252°	198°	216°	234°	252°	198°	216°	234°	252°
0.5	0.146	0.161	0.175	0.188	0.067	0.091	0.110	0.130	-0.155	-0.137	-0.114	-0.107	-0.245	-0.241	-0.233	-0.233	0.078	0.101	0.129	0.163				
14.0	-.007	-.010	-.008	-.008	-.012	-.016	-.016	-.012	-.021	-.025	-.025	-.023	-.026	-.029	-.029	-.028	-.011	-.025	-.035	-.035				
43.0	-.006	-.008	-.012	-.015	-.007	-.010	-.014	-.016	-.010	-.012	-.016	-.019	-.012	-.012	-.016	-.009	-.010	-.016	-.024	-.035				

TABLE V - EXTERNAL AND INTERNAL PRESSURE COEFFICIENTS OF NACA 8-INCH RAM-JET CONFIGURATION  
FOR FOUR ANGLES OF ATTACK AT FREE-STREAM MACH NUMBER OF 1.99 - Concluded



Station	$\alpha = 60^\circ; m_3/m_0 = 0.975$				$\alpha = 60^\circ; m_3/m_0 = 0.871$				$\alpha = 10^\circ; m_3/m_0 = 0.955$				$\alpha = 10^\circ; m_3/m_0 = 0.851$			
	(a) Concluded. Longitudinal distribution of $C_p$ .															
	Outer shell		Center body	Outer shell		Center body	Outer shell		Center body	Outer shell		Center body	Outer shell		Center body	
	External	Internal		External	Internal		External	Internal		External	Internal		External	Internal		
$\theta \rightarrow$	180°	270°	0°	0°	180°	270°	0°	0°	180°	270°	0°	0°	180°	270°	0°	0°
-1.0			0.639				0.638			0.788			0.757			
-0.5			.639				.658			.785			.785			
0			.640				1.274			.778			.785			
0.5	0.029	0.218	0.699	.477	-0.052	0.154	1.210	.912	-0.024	0.213	0.248	.423	-0.170	0.176	0.879	0.785
1.0	.012	.164	.669	.608	-.029	.155	1.240	1.197	-.053	.155	.442	.560	-.141	.157	1.062	1.006
1.5	-.007	.151	1.087	1.114	-.026	.115	1.283	1.274	.128	.357	.232	.130	.131	1.168	1.167	
2.0	-.016	.104	1.129	1.141	-.029	.090	1.304	1.306	-.067	.100	.344	-.006	.106	1.216	1.215	
2.5	-.024	.092	1.169	1.165	-.034	.080	1.318	1.323		.094	.256	.074	.092	1.246	1.247	
3.0	-.031	.075	1.188	1.185	-.042	.062	1.352	1.335		.065	.141	.314	.074	1.289	1.289	
4.0	-.042	.047	1.202	1.210	-.052	.041	1.344	1.356		.033	.466	.242	.042	1.297	1.307	
5.0	-.041	.030	1.203	1.205	-.049	.084	1.352	1.358		-.067	.012	.688	.722	-.094	.020	1.514
6.0	-.045	.008	1.200	1.184	-.062	.006	1.354	1.344		-.060	-.009	.804	.780	-.082	-.005	1.326
7.0	-.049	-.006	1.194	1.189	-.066	-.010	1.347	1.347		.001	-.027	.824	.807	-.004	-.023	1.381
8.0	-.036	-.012	1.214	1.194	-.042	-.015	1.361	1.347		-.038	-.036	.847	.828	-.056	-.054	1.345
9.0	-.034	-.024	1.223	1.258	-.038	-.025	1.368	1.378		-.034	-.046	.845	.870	-.047	-.048	1.351
10.0	-.043	-.050		1.282	-.060	-.026		1.384	-.041	-.048		.861	-.056	-.048		1.370
11.0	-.084	-.053		1.274	-.029	-.004		1.396	-.019	-.062		.902	-.082	-.062		1.394
12.0	-.017	-.031		1.308	-.023	-.036		1.417	-.012	-.067		.968	-.024	-.069		1.405
14.0	-.010	-.033		1.377	-.014	-.058		1.460	-.002	-.079		1.079	-.014	-.082		1.444
16.0	-.004	-.036		1.453	-.007	-.040		1.498	-.008	-.089		1.165	-.007	-.085		1.478
18.0	.005	-.036		1.480	-.002	-.038		1.527	-.017	-.096		1.231	-.008	-.098		1.509
21.0	.081	-.035		1.543	.016	-.039		1.587	.018	-.108		1.314	.006	-.110		1.551
24.0	.003	-.038		1.599	.001	-.029		1.605	.006	-.111		1.394	-.002	-.116		1.569
27.0	-.011	-.036		1.640	-.014	-.028		1.640	-.005	-.110		1.445	-.009	-.116		1.580
31.0	.002			1.668	.002			1.681	.012			1.478	.008			1.642
35.0	-.020				-.021				-.016				-.019			
37.0				1.697				1.695		.001		1.608	-.002			1.668
40.0	-.006				-.006				-.004				-.006			
45.0	-.005				-.006											

(b) Concluded. Circumferential distribution of $C_p$ .																
Station	Outer shell, external				Outer shell, external				Outer shell, external				Outer shell, external			
$\theta \rightarrow$	198°	216°	234°	252°	198°	216°	234°	252°	198°	216°	234°	252°	198°	216°	234°	252°
0.5	0.063	0.074	0.124	0.164	-0.031	0.005	0.045	0.088	0	0.037	0.055	0.139	-0.147	-0.102	-0.057	0.061
14.0	-.015	-.026	-.035	-.058	-.019	-.069	-.058	-.042	-.014	-.046	-.090	-.102	-.027	-.053	-.096	-.111
45.0	-.011	-.016	-.024	-.038	-.012	-.017	-.034	-.036	-.028	-.046	-.044	-.056	-.027	-.046	-.046	-.057

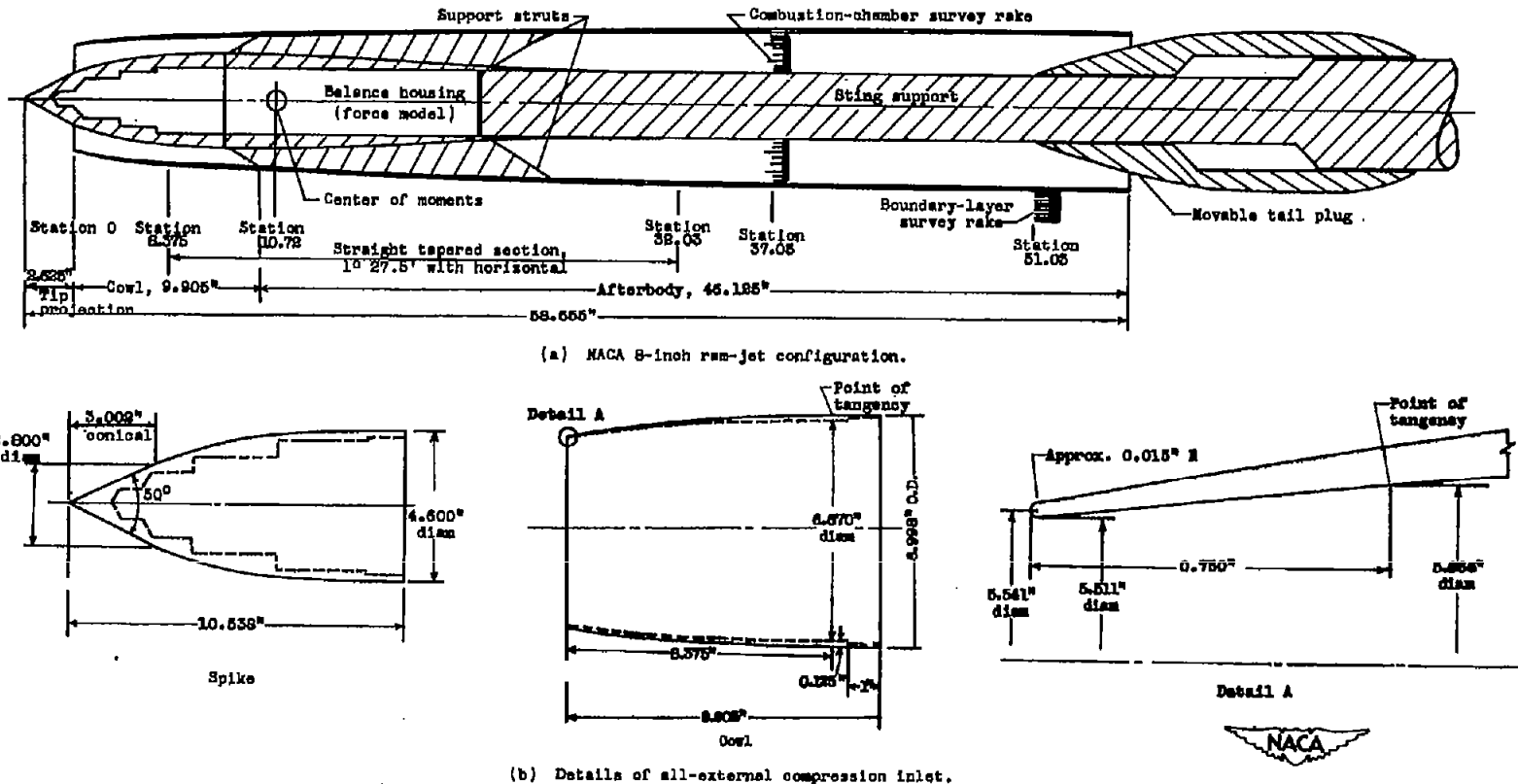


Figure 1. - Schematic diagram of NASA 8-inch ram-jet configuration showing principal dimensions of model and details of all-external compression inlet.

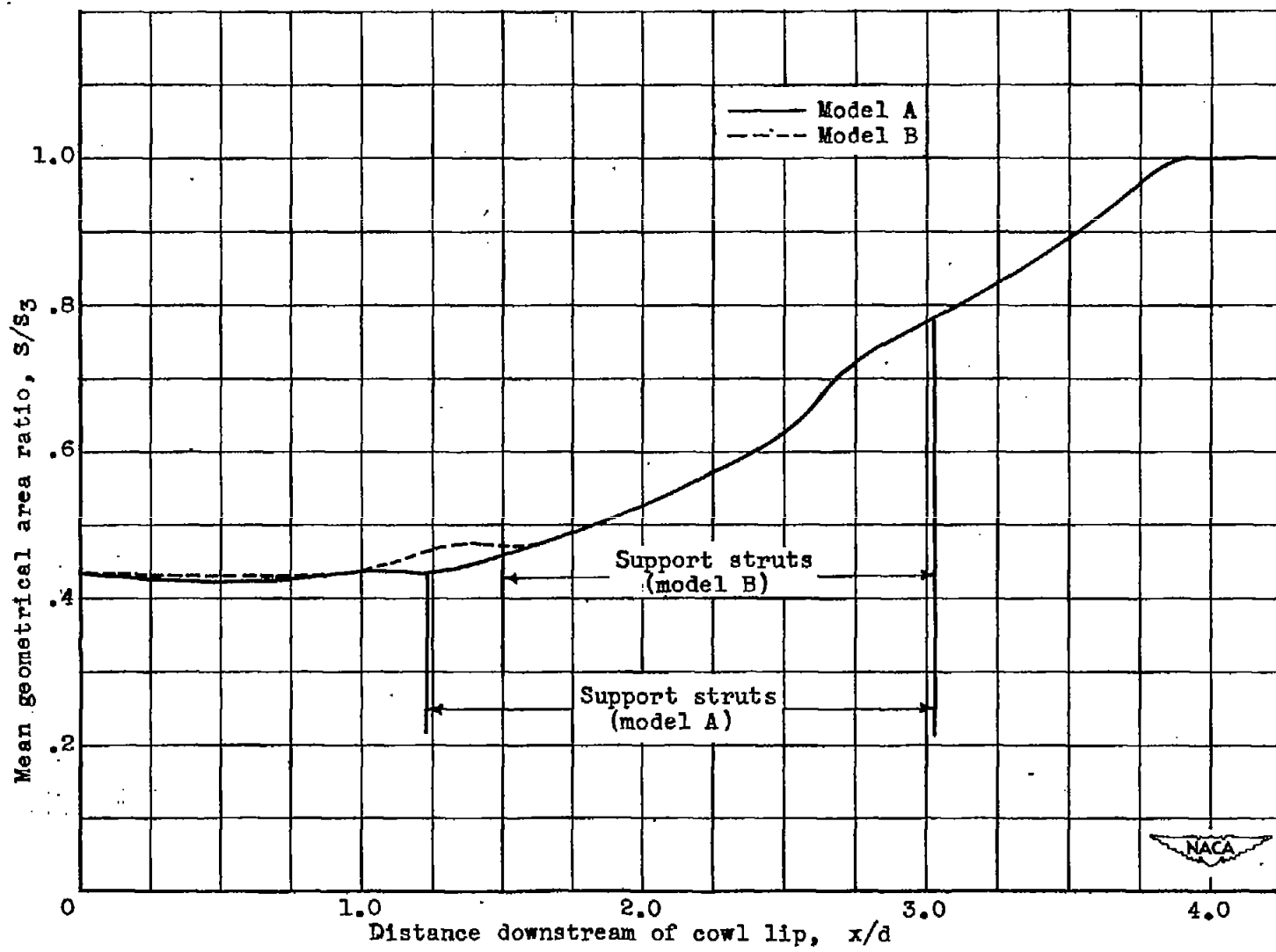


Figure 2. - Longitudinal variation of mean geometrical area.

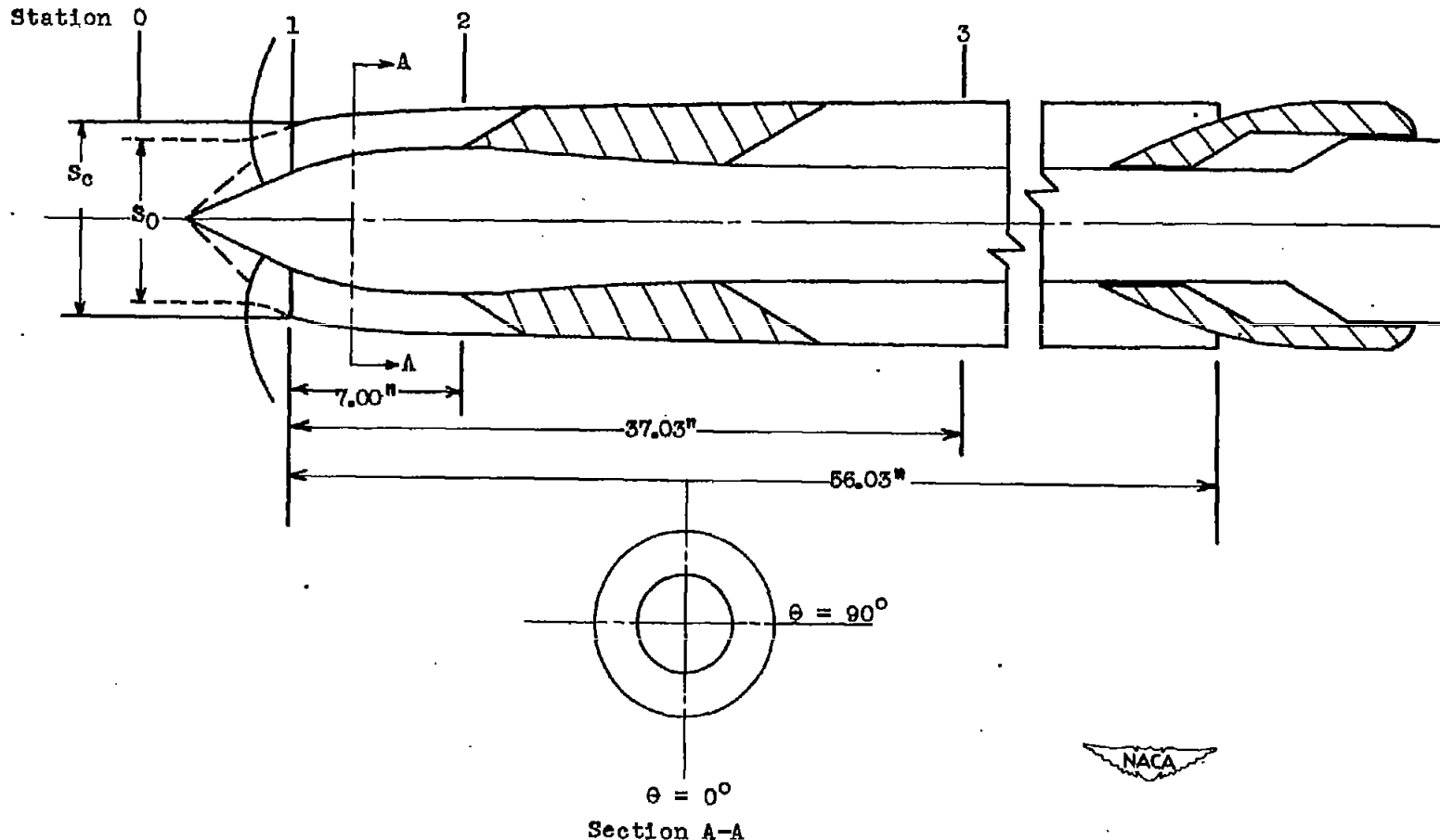


Figure 3. - Notation for 8-inch ram-jet configuration.

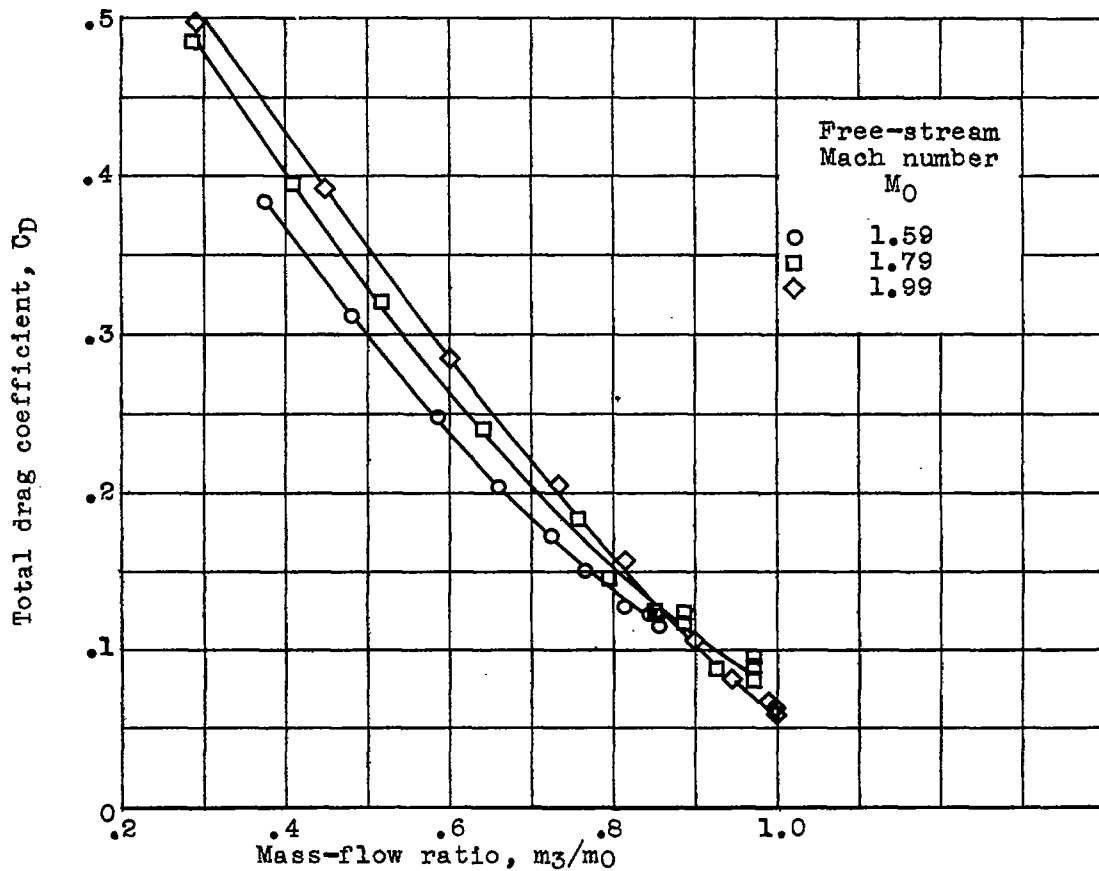


Figure 4. - Variation of total drag coefficient with mass-flow ratio at zero angle of attack for three Mach numbers. Model B.

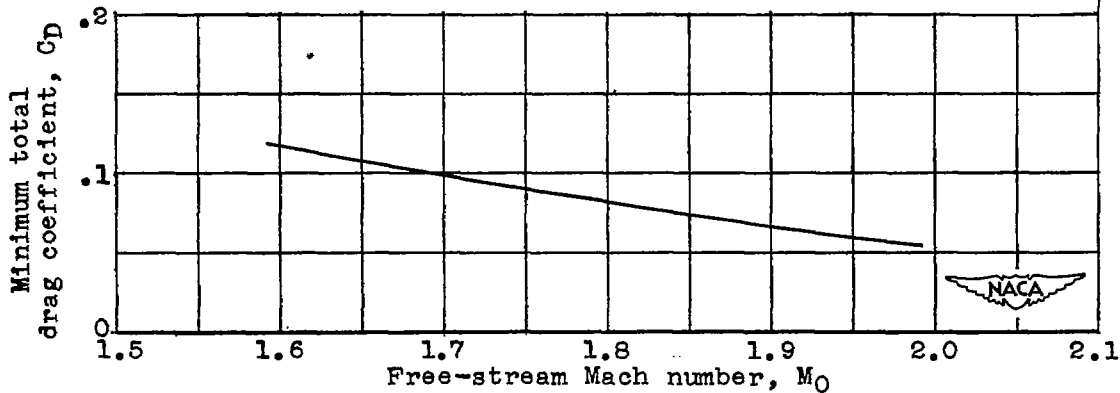
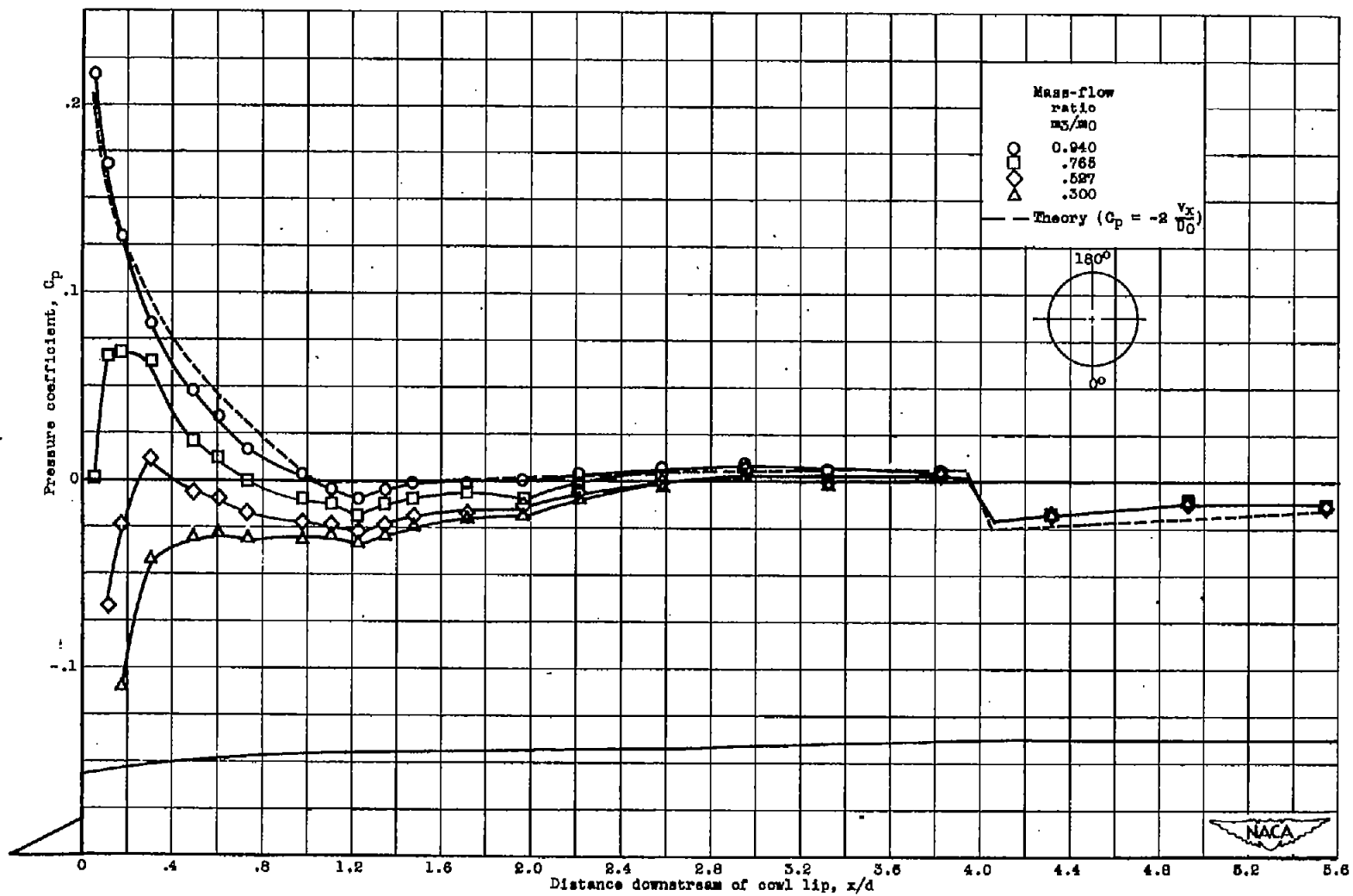


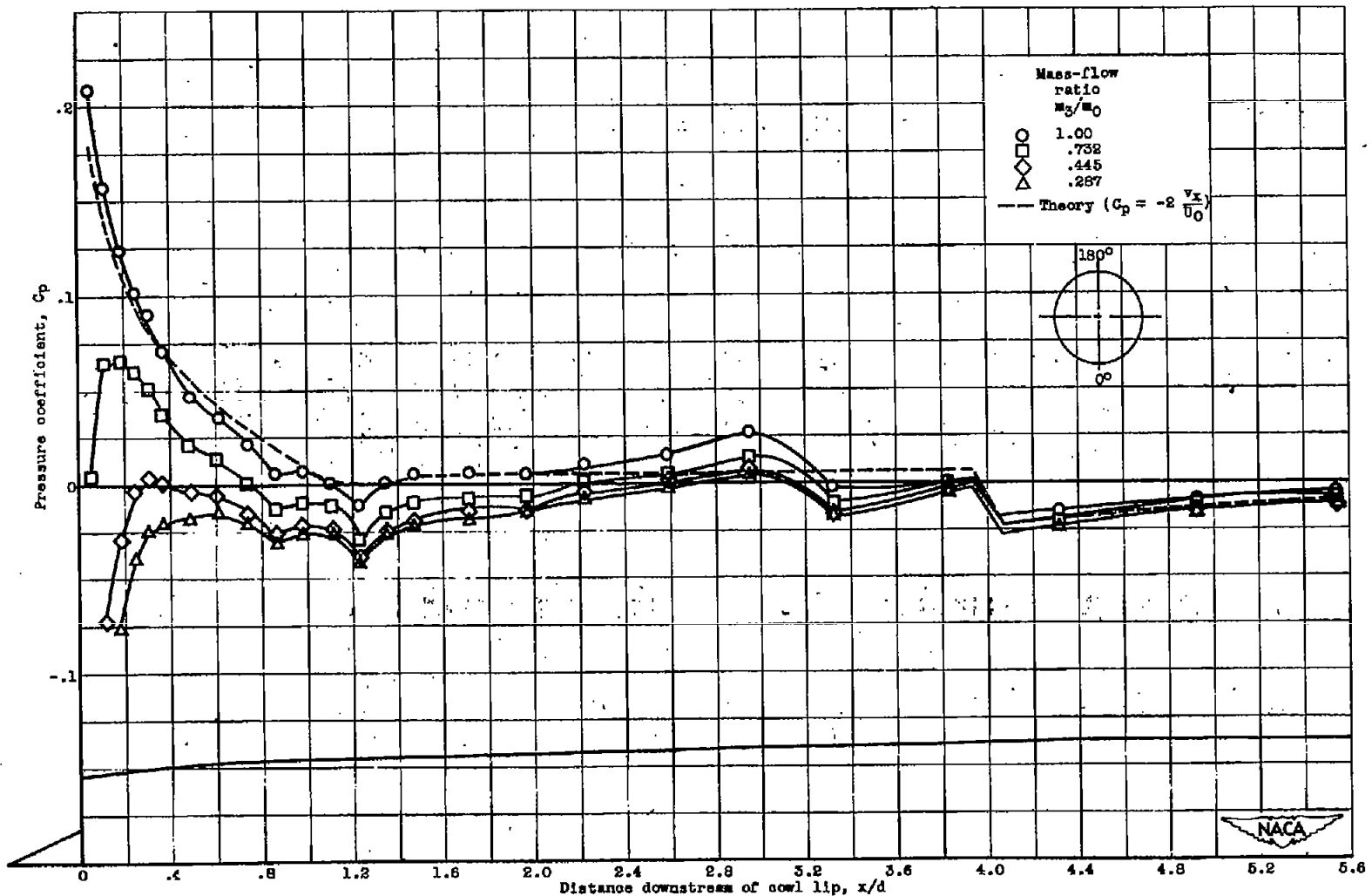
Figure 5. - Variation of minimum drag coefficient with free-stream Mach number at zero angle of attack. Model B.

2029



(a) Free-stream Mach number, 1.79.

Figure 6. - Longitudinal variation of external pressure coefficient at zero angle of attack for a range of mass-flow ratios at two Mach numbers.  
 $\alpha = 180^\circ$ .



(b) Free-stream Mach number, 1.99.

Figure 6. - Concluded. Longitudinal variation of external pressure coefficient at zero angle of attack for a range of mass-flow ratios at two Mach numbers.  $\theta = 180^\circ$ .

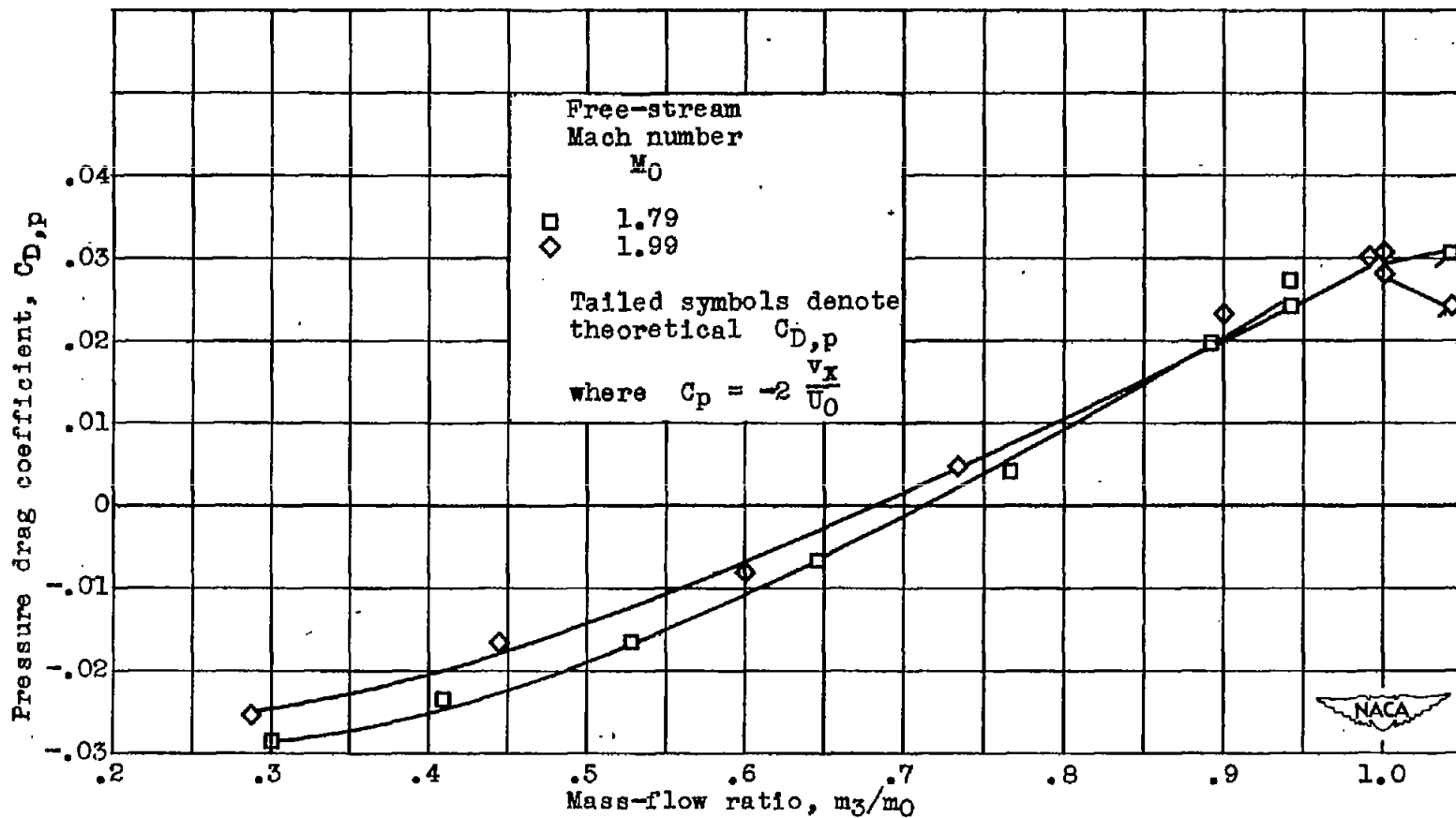


Figure 7. — Variation of pressure drag coefficient with mass-flow ratio at zero angle of attack for two Mach numbers.

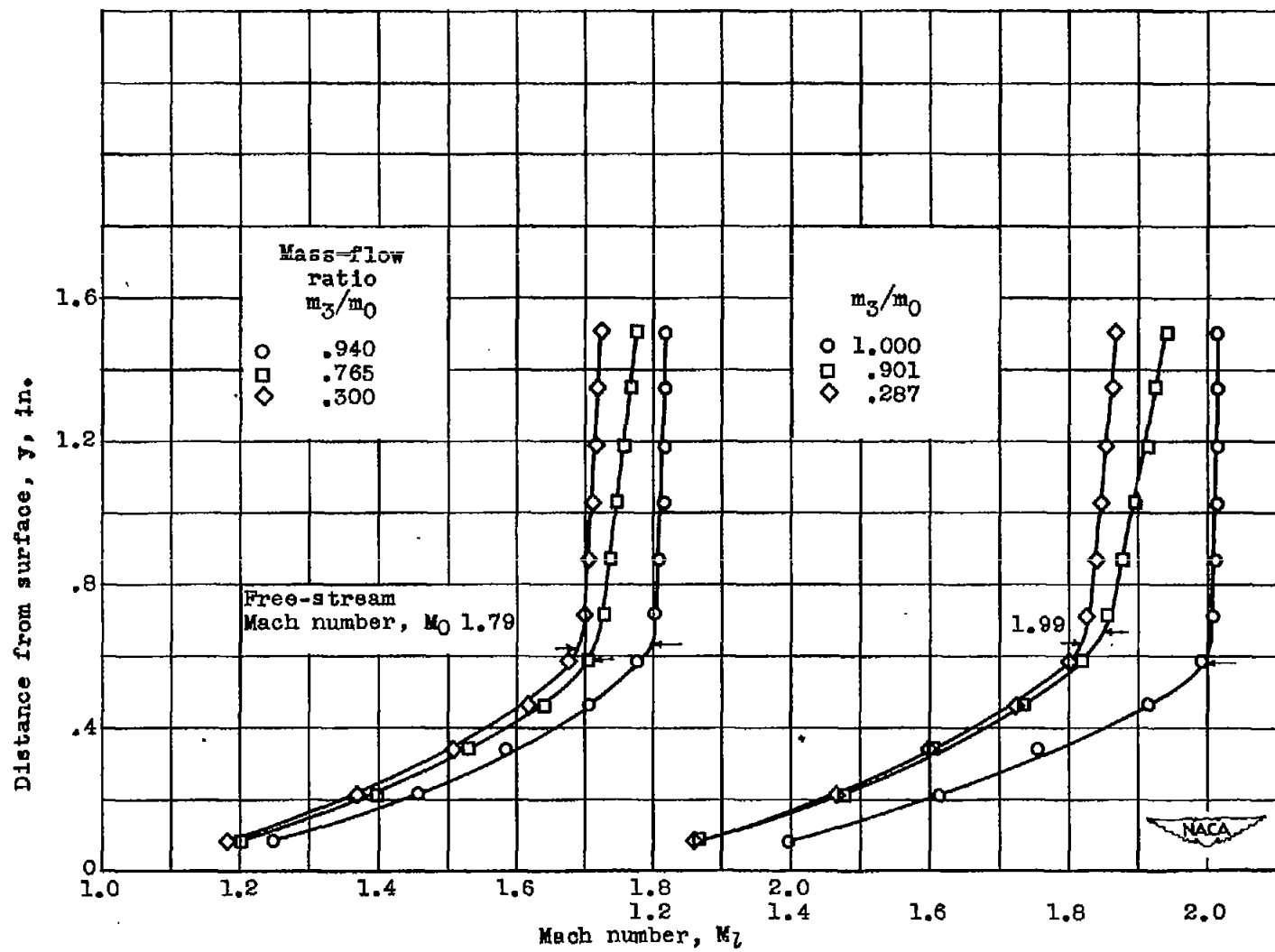


Figure 8. - Variation of Mach-number distribution in boundary layer at zero angle of attack for range of mass-flow ratios at two Mach numbers. Station 51.03.

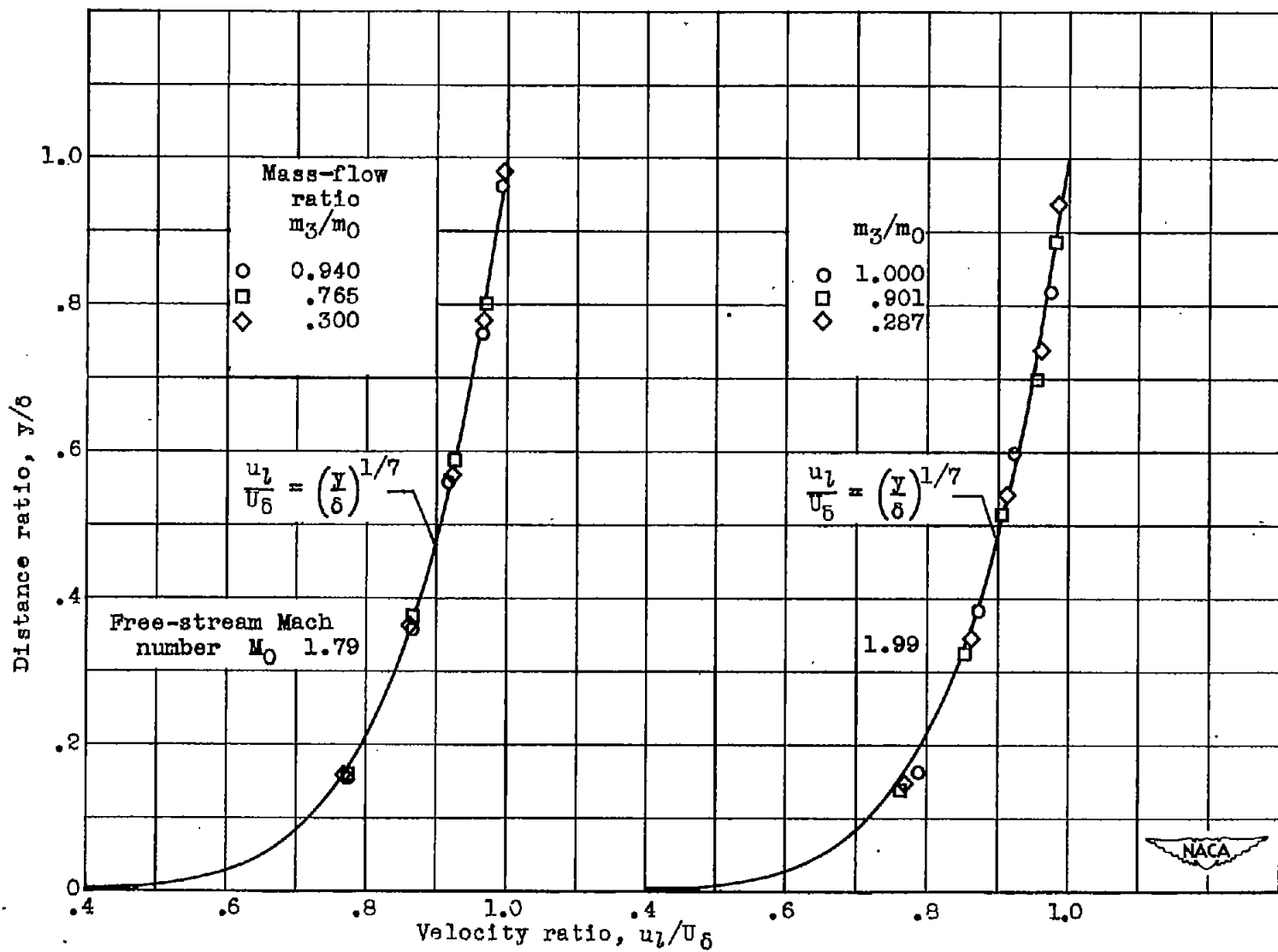


Figure 9. - Comparison of experimental and power-law boundary-layer profiles at zero angle of attack for range of mass-flow ratios and two Mach numbers.

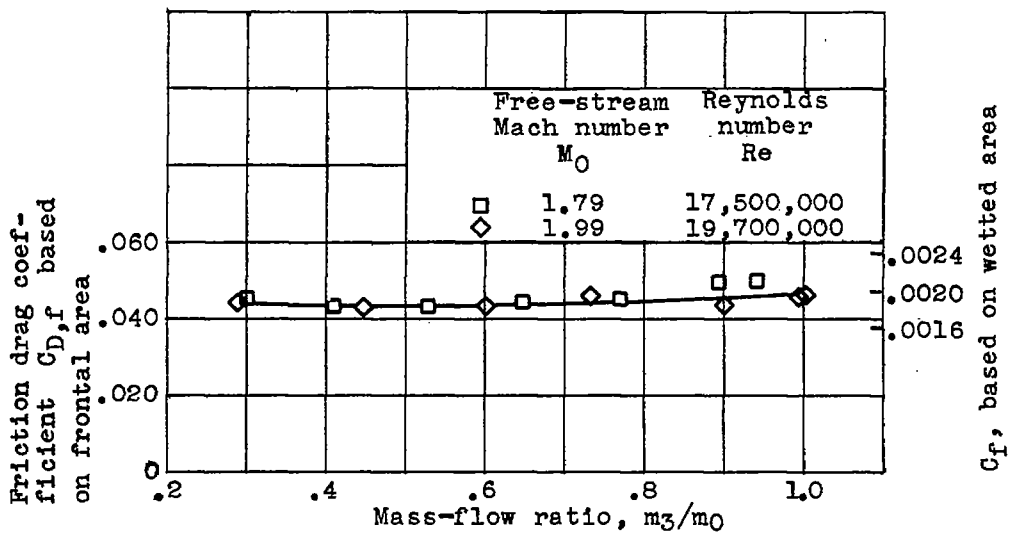


Figure 10. - Variation of friction drag coefficient with mass-flow ratio at zero angle of attack for two Mach numbers.

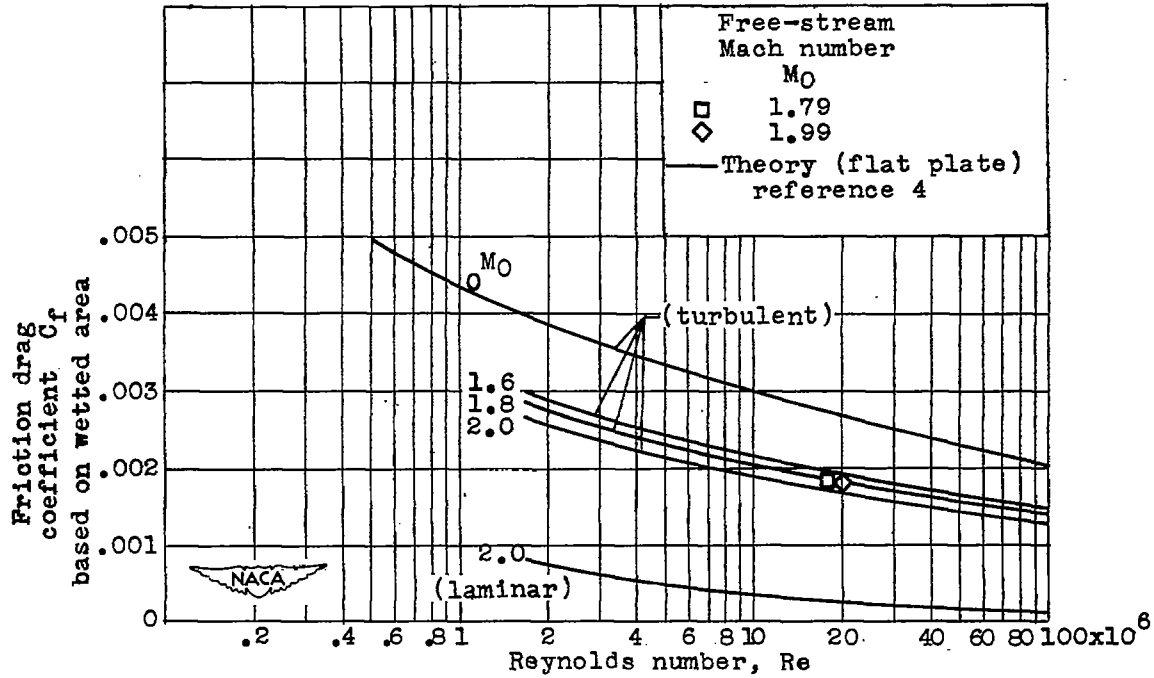


Figure 11. - Comparison of experimental skin-friction drag coefficients with two-dimensional compressible flow theory at two Mach numbers.

2039

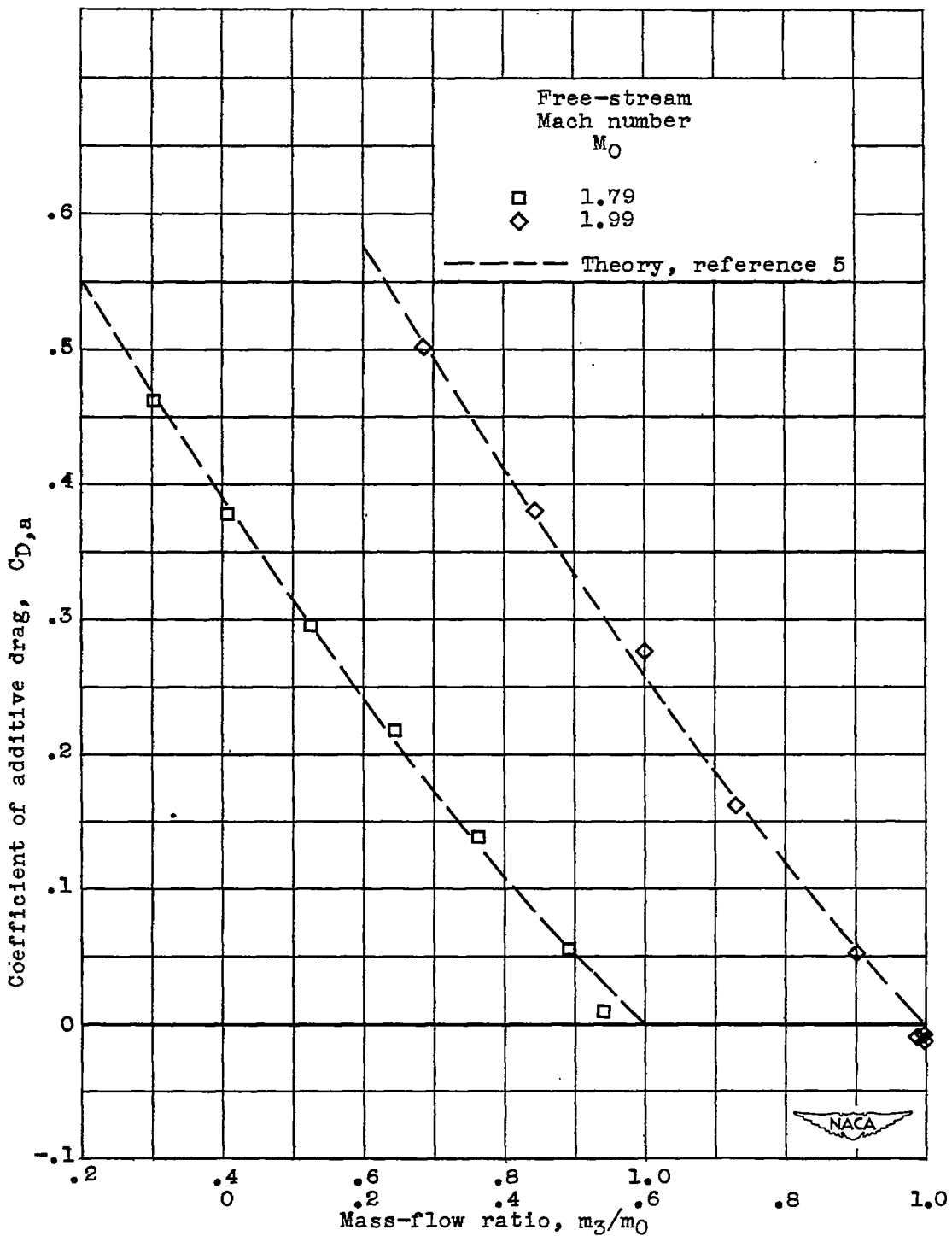


Figure 12. - Comparison of experimental additive drag coefficients with one-dimensional theory for range of mass-flow ratios at two Mach numbers.

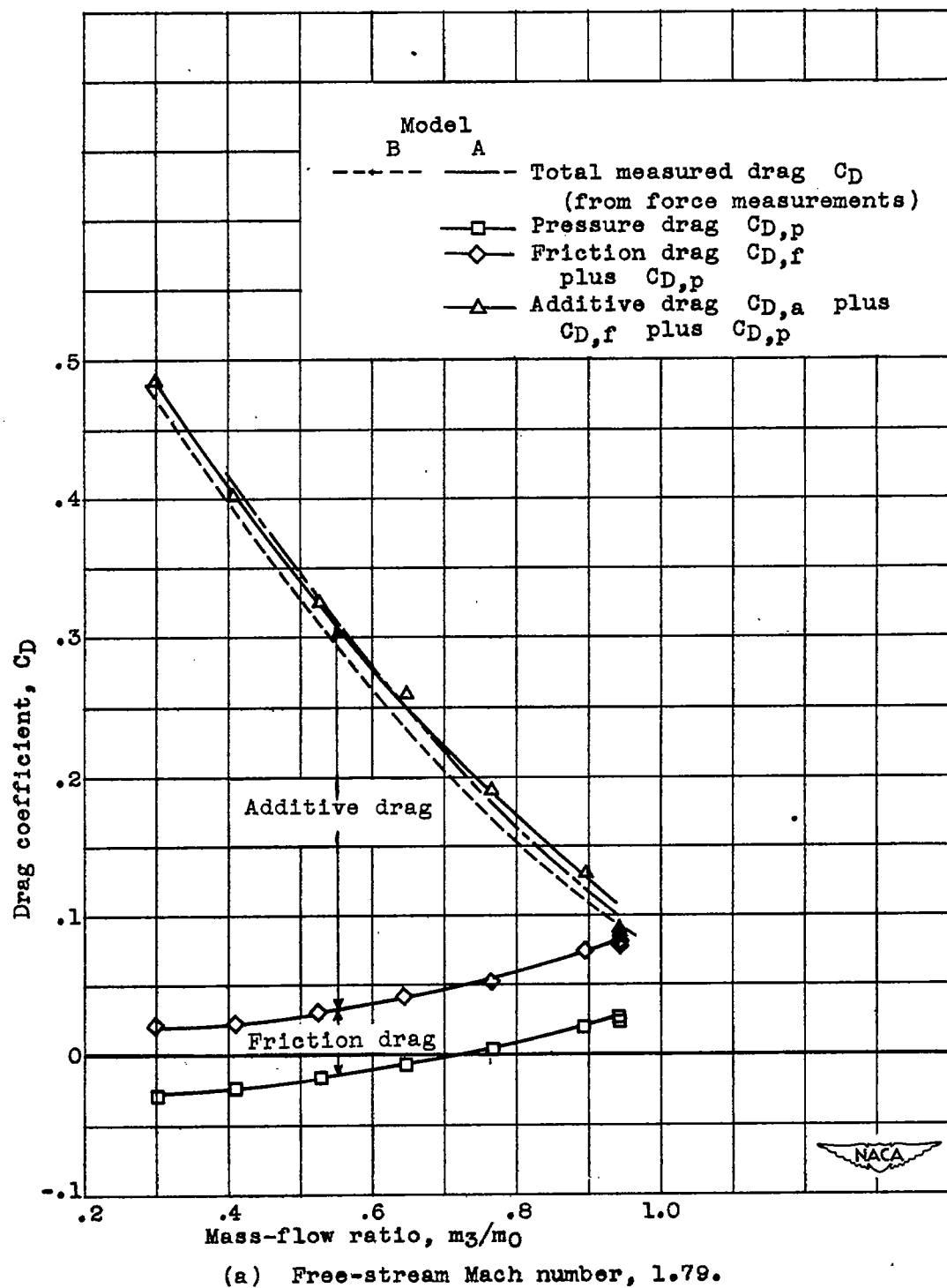
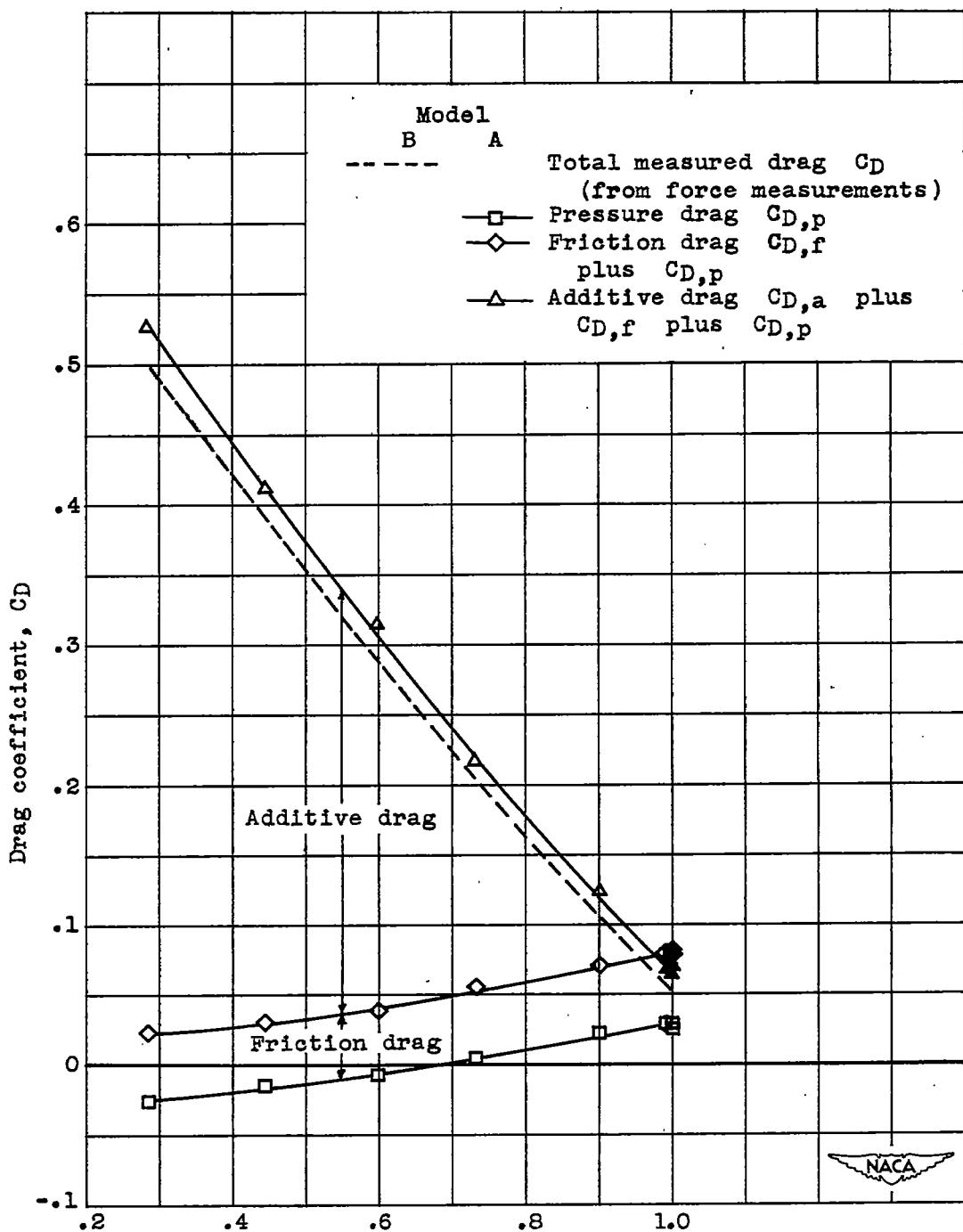


Figure 13. - Variation of components of total drag coefficients with mass-flow ratio at zero angle of attack for two Mach numbers.



(b) Free-stream Mach number, 1.99.

Figure 13. - Concluded. Variation of components of total drag coefficients with mass-flow ratio at zero angle of attack for two Mach numbers.

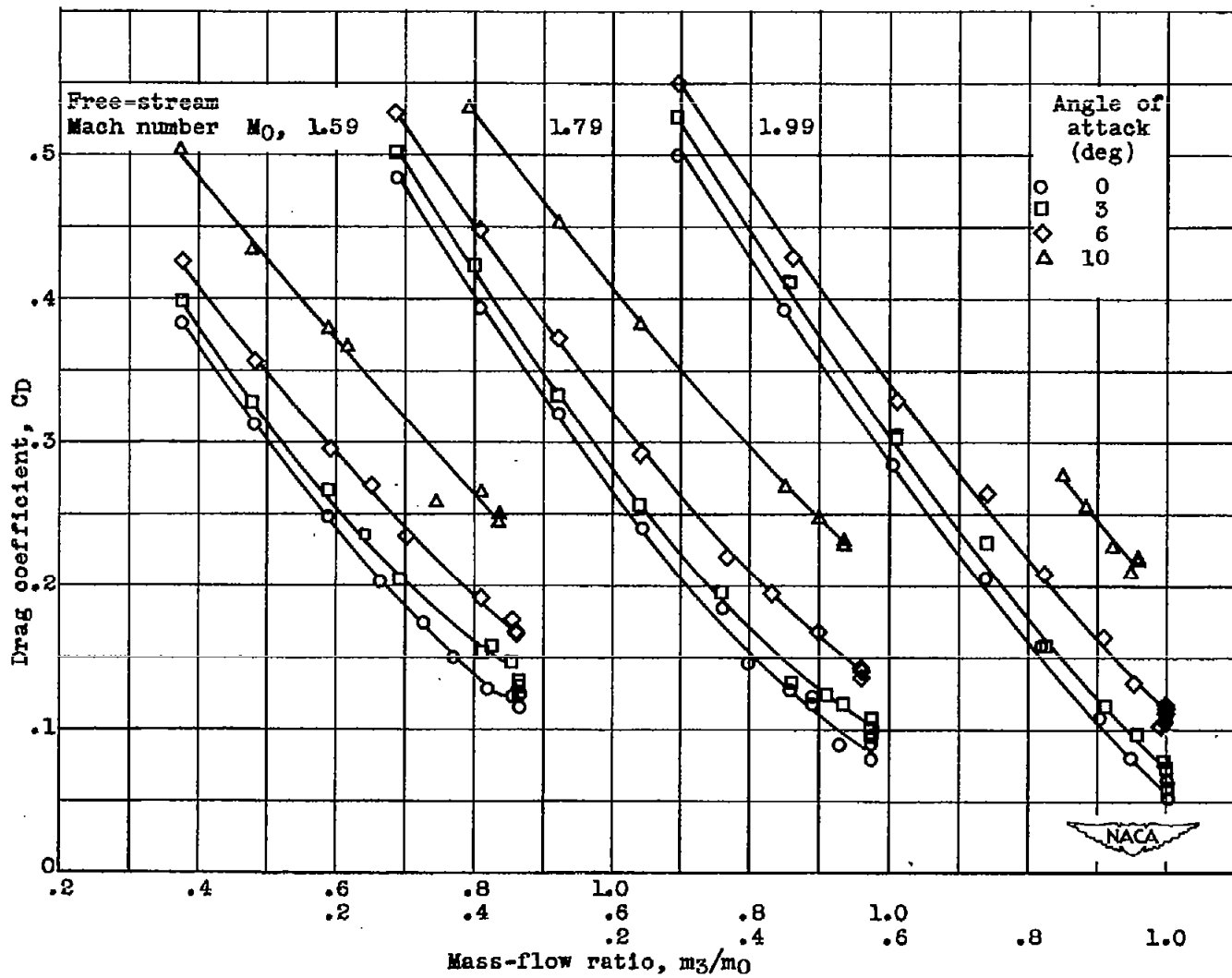


Figure 14. - Variation of total drag coefficient with mass-flow ratio at four angles of attack for three Mach numbers. Model B.

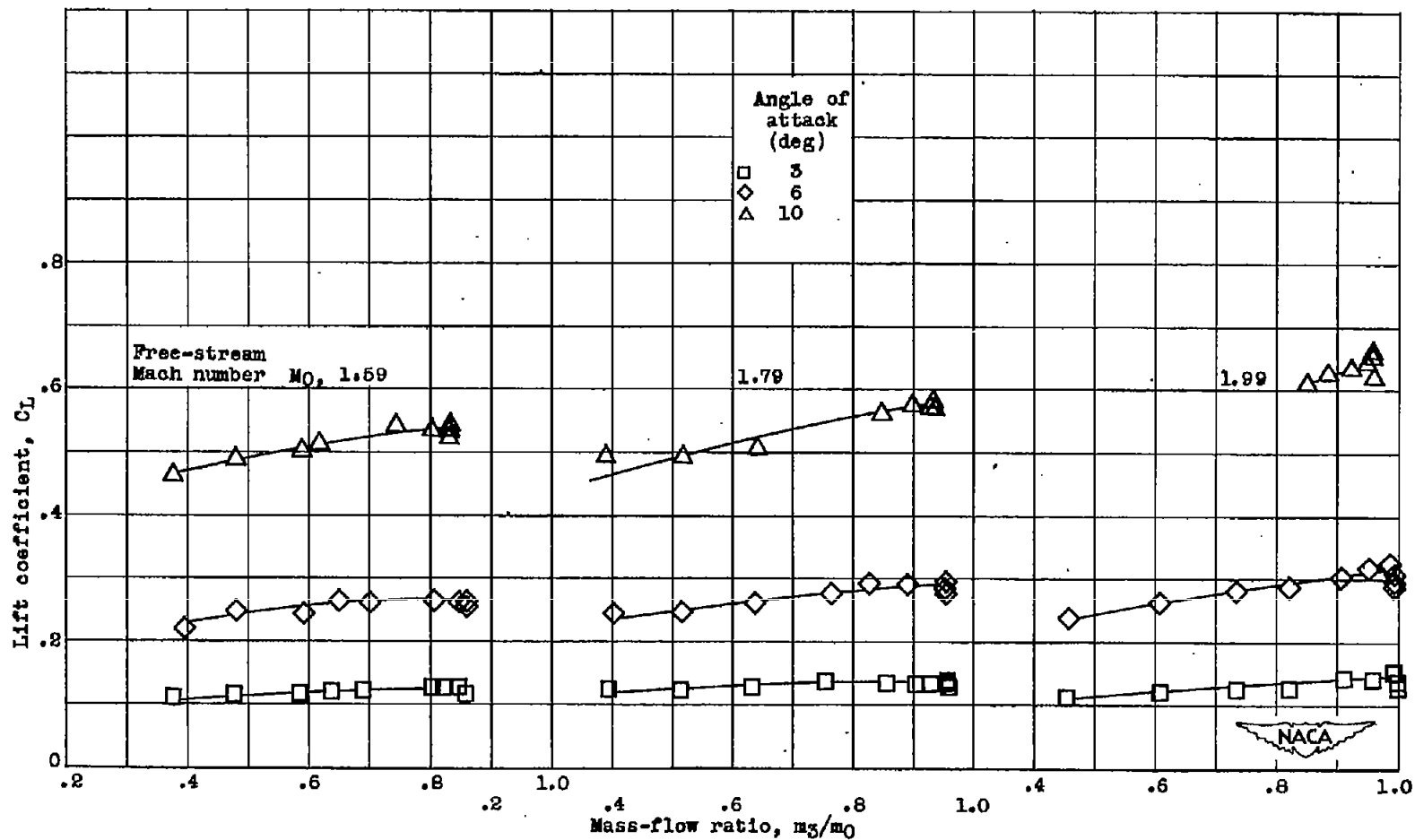


Figure 15. - Variation of external lift coefficients with mass-flow ratio at three angles of attack for three Mach numbers. Model B.

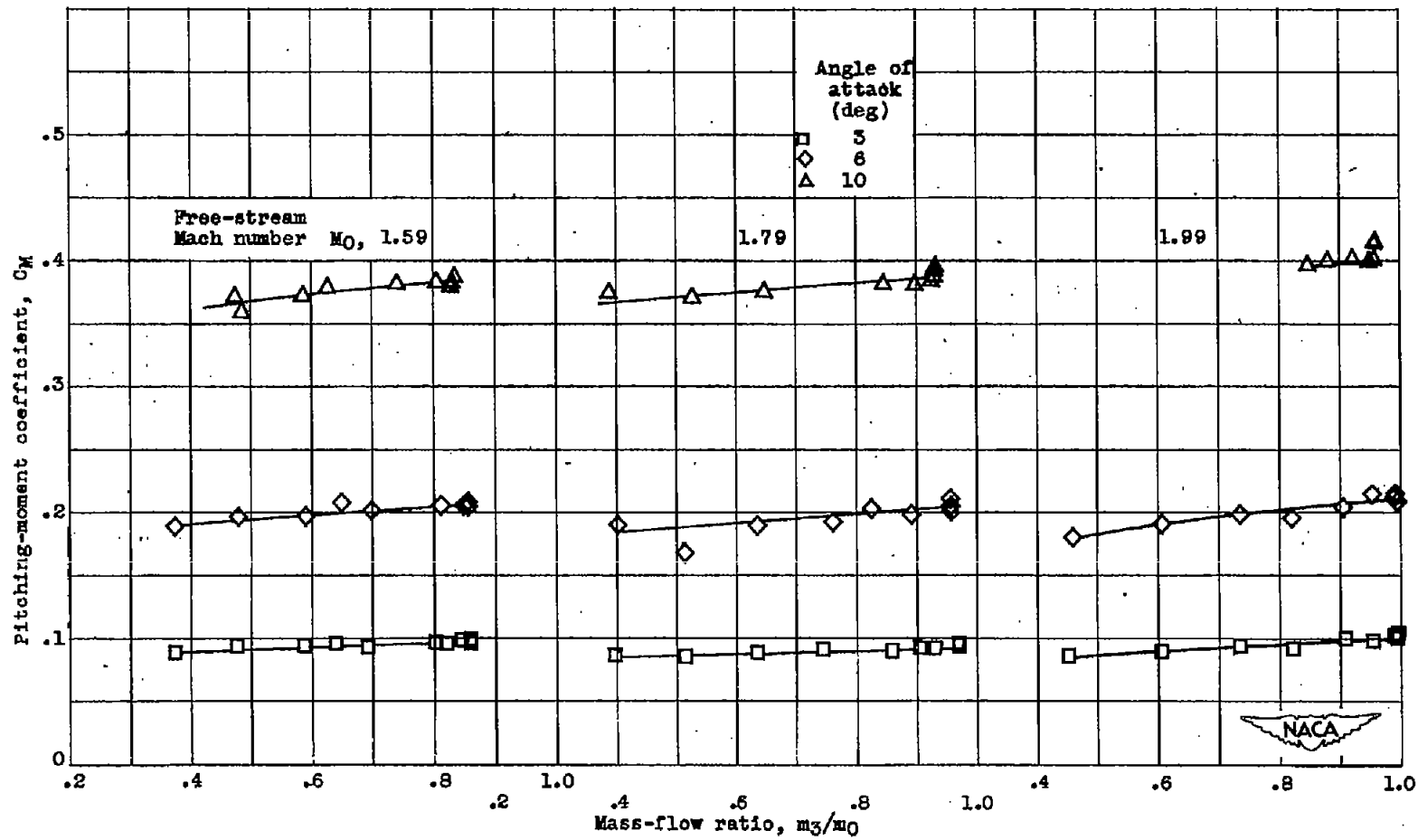


Figure 16. - Variation of pitching-moment coefficient about base of model with mass-flow ratio at three angles of attack for three Mach numbers. Model B.

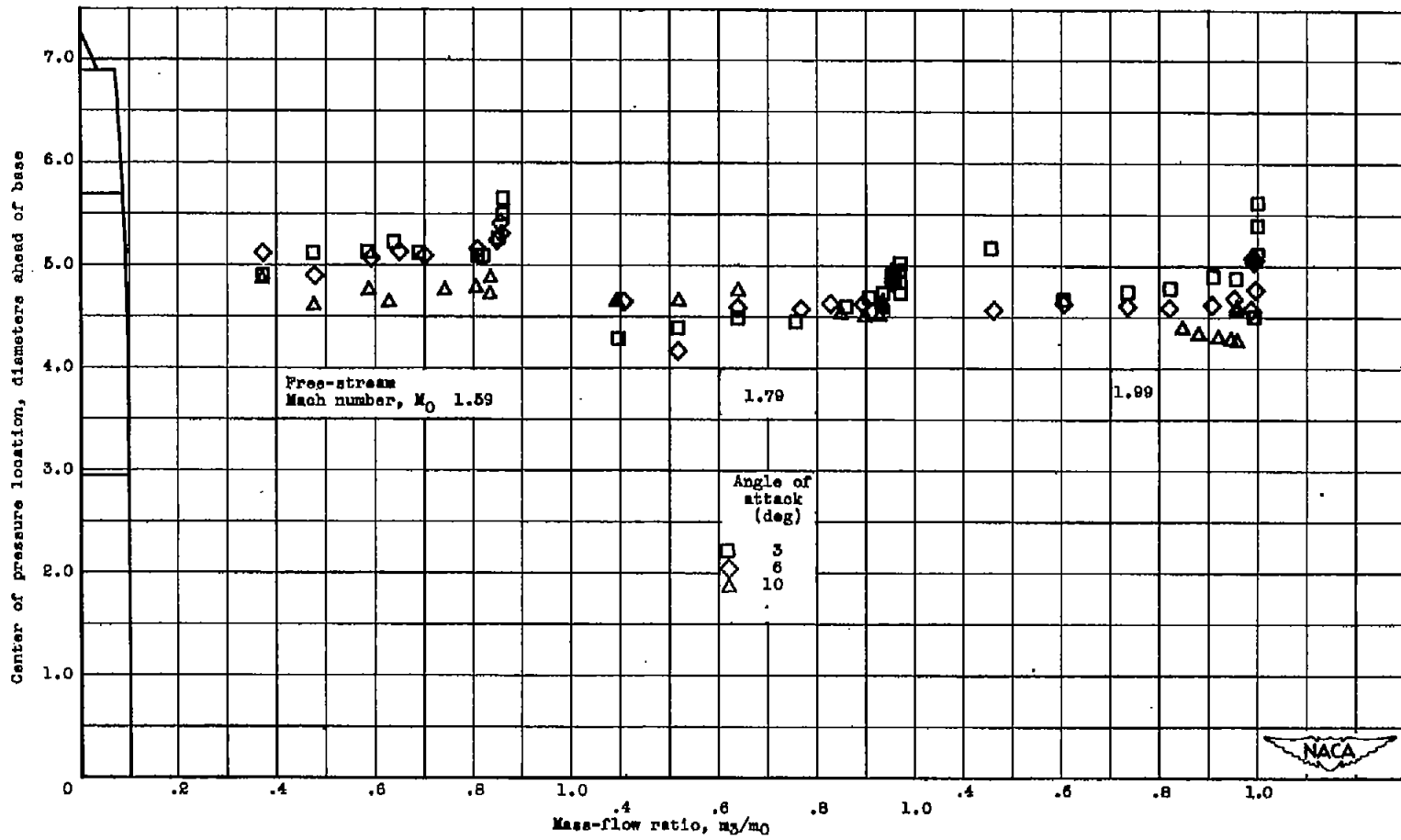


Figure 17. - Variation of center of pressure location with mass-flow ratio at three angles of attack for three Mach numbers. Model B.

2039

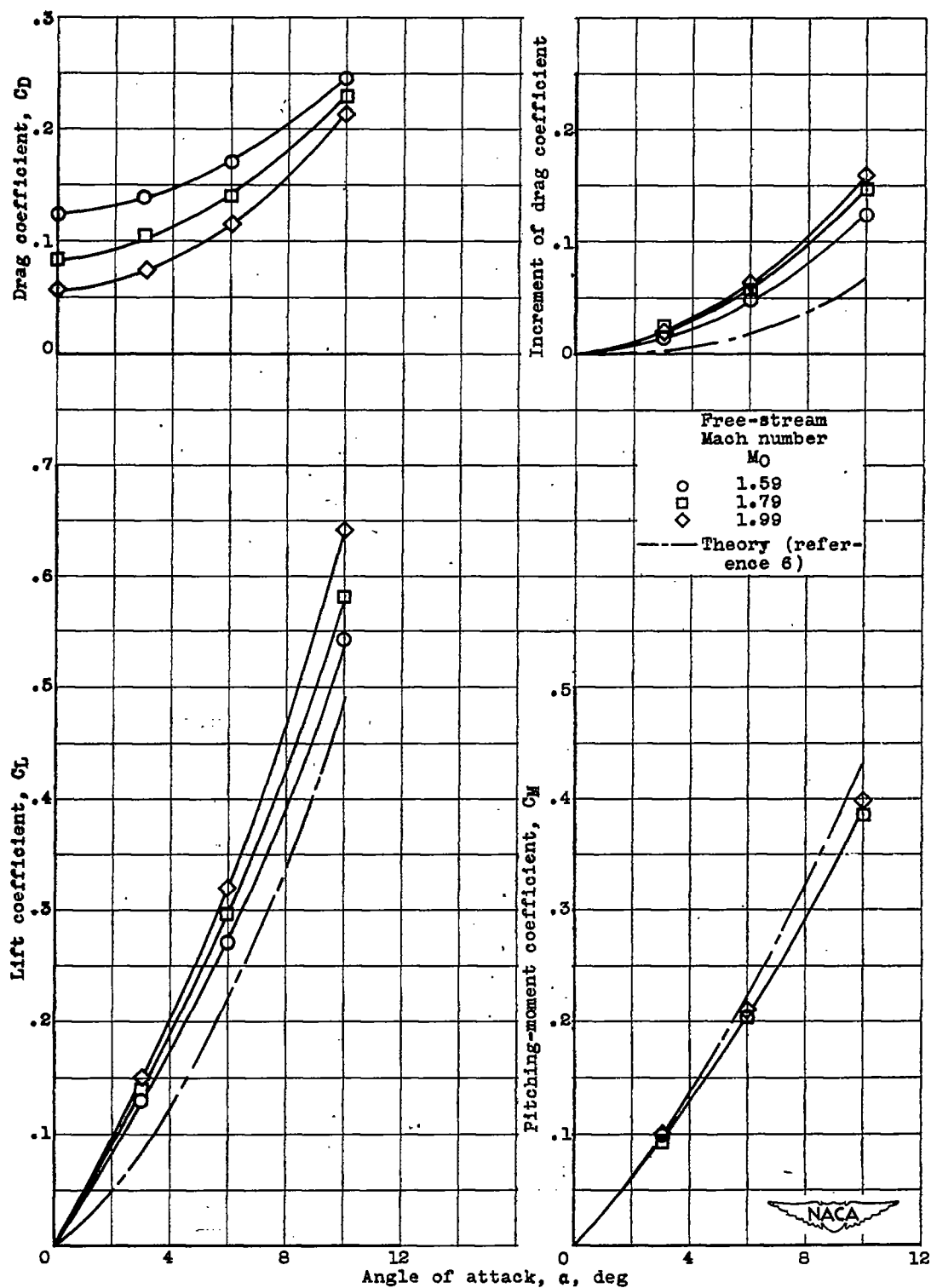


Figure 18. - Variation of external aerodynamic coefficients with angle of attack at critical mass-flow ratios for three Mach numbers. Model B.

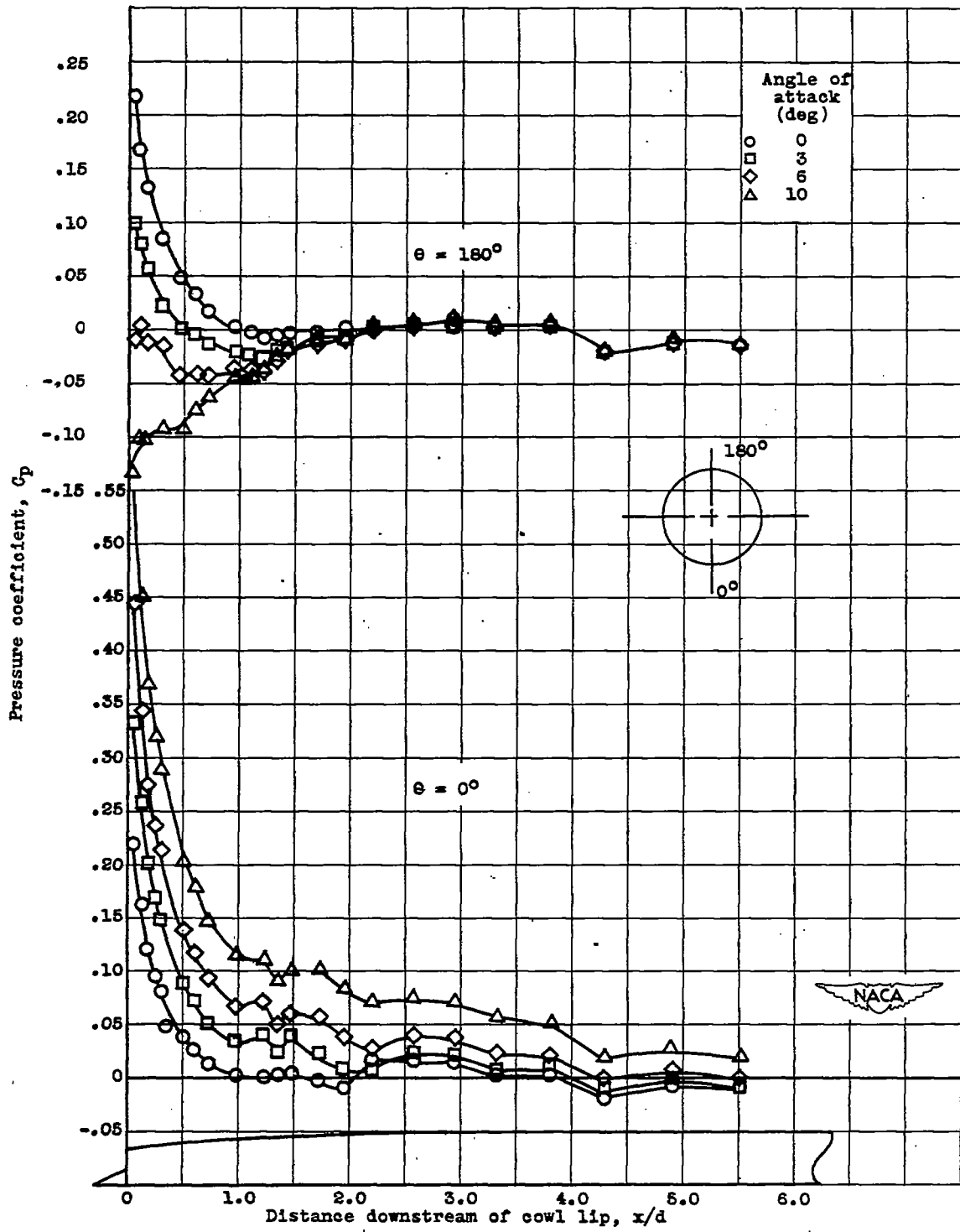


Figure 19. - Longitudinal variation of external pressure coefficients at constant mass-flow ratio of 0.940 for four angles of attack. Free-stream Mach number 1.79.

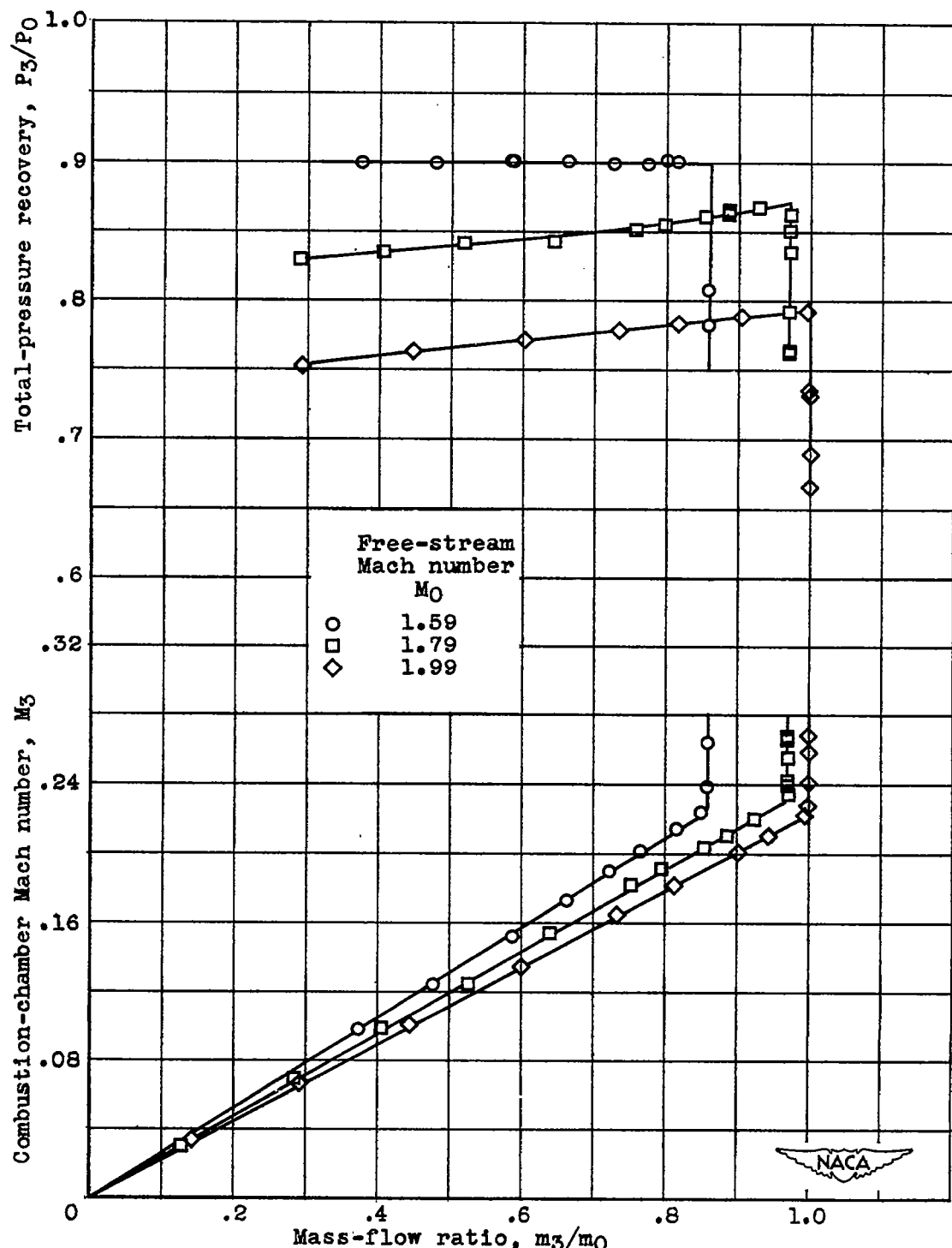


Figure 20. - Variation of total-pressure recovery and combustion-chamber Mach number with mass-flow ratio at zero angle of attack for three Mach numbers. Model B.

2029

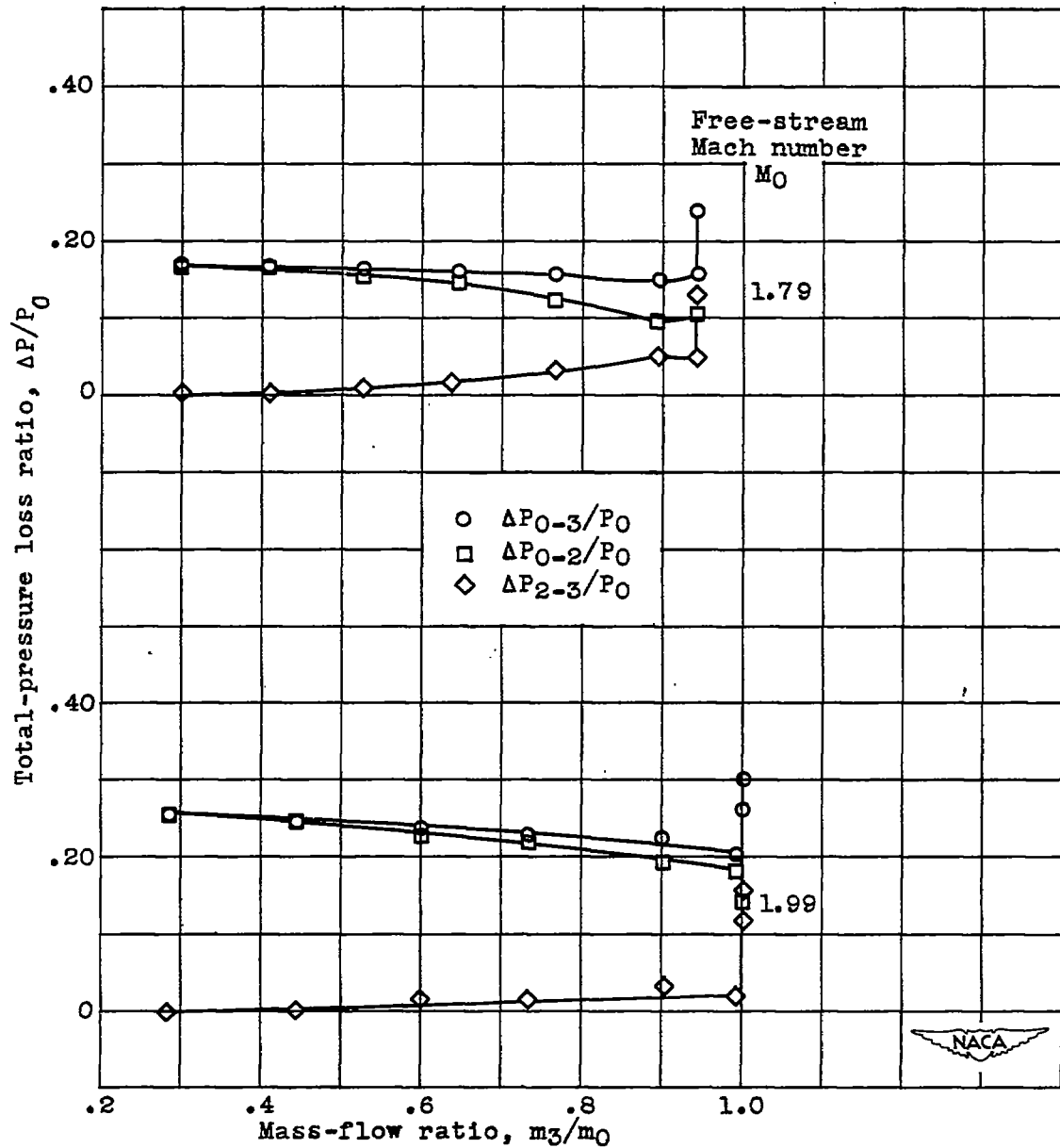


Figure 21. - Variation of components of total-pressure loss with mass-flow ratio at zero angle of attack for two Mach numbers.

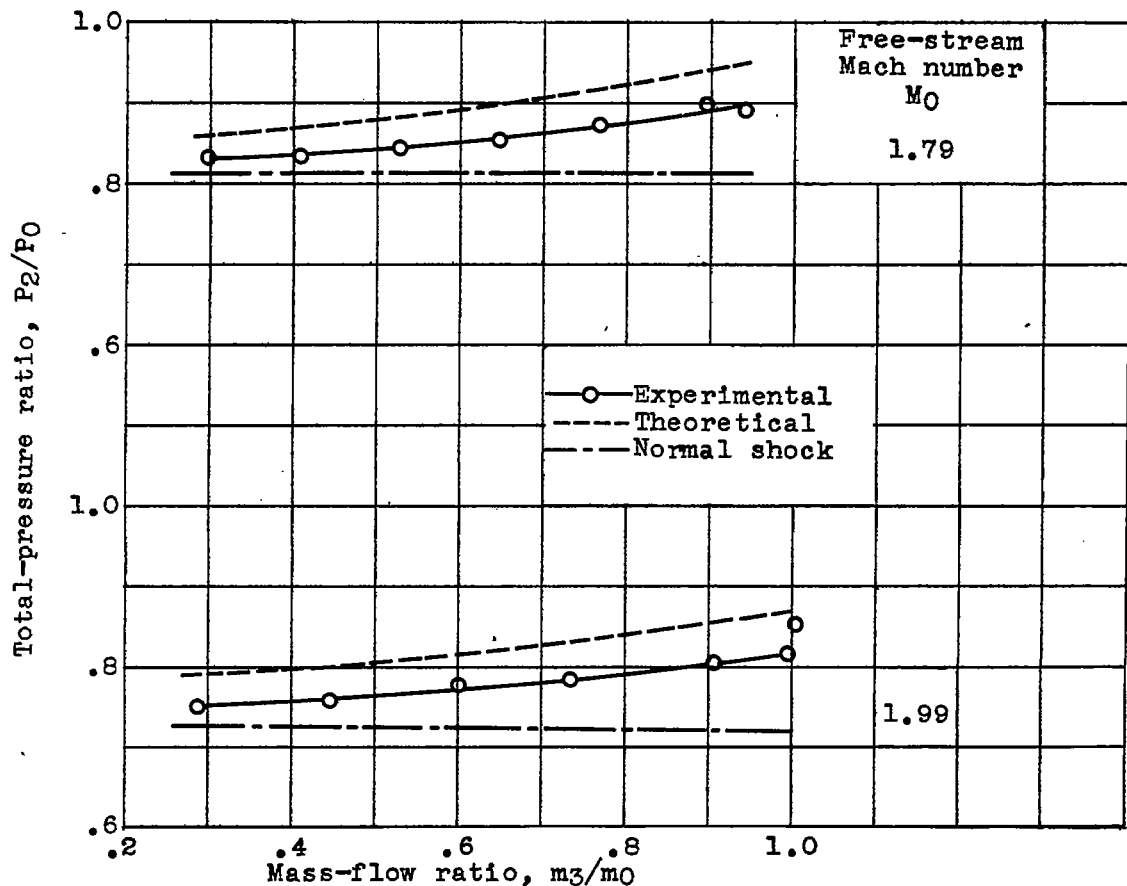


Figure 22. - Comparison of experimental inlet losses with theory at zero angle of attack for range of mass-flow ratios at two Mach numbers.

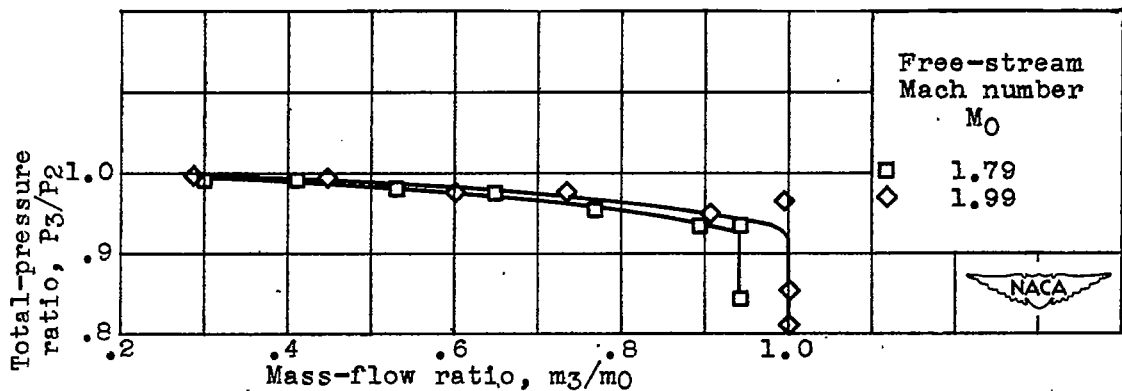


Figure 23. - Variation of subsonic-diffuser recovery with mass-flow ratio at zero angle of attack for two Mach numbers.

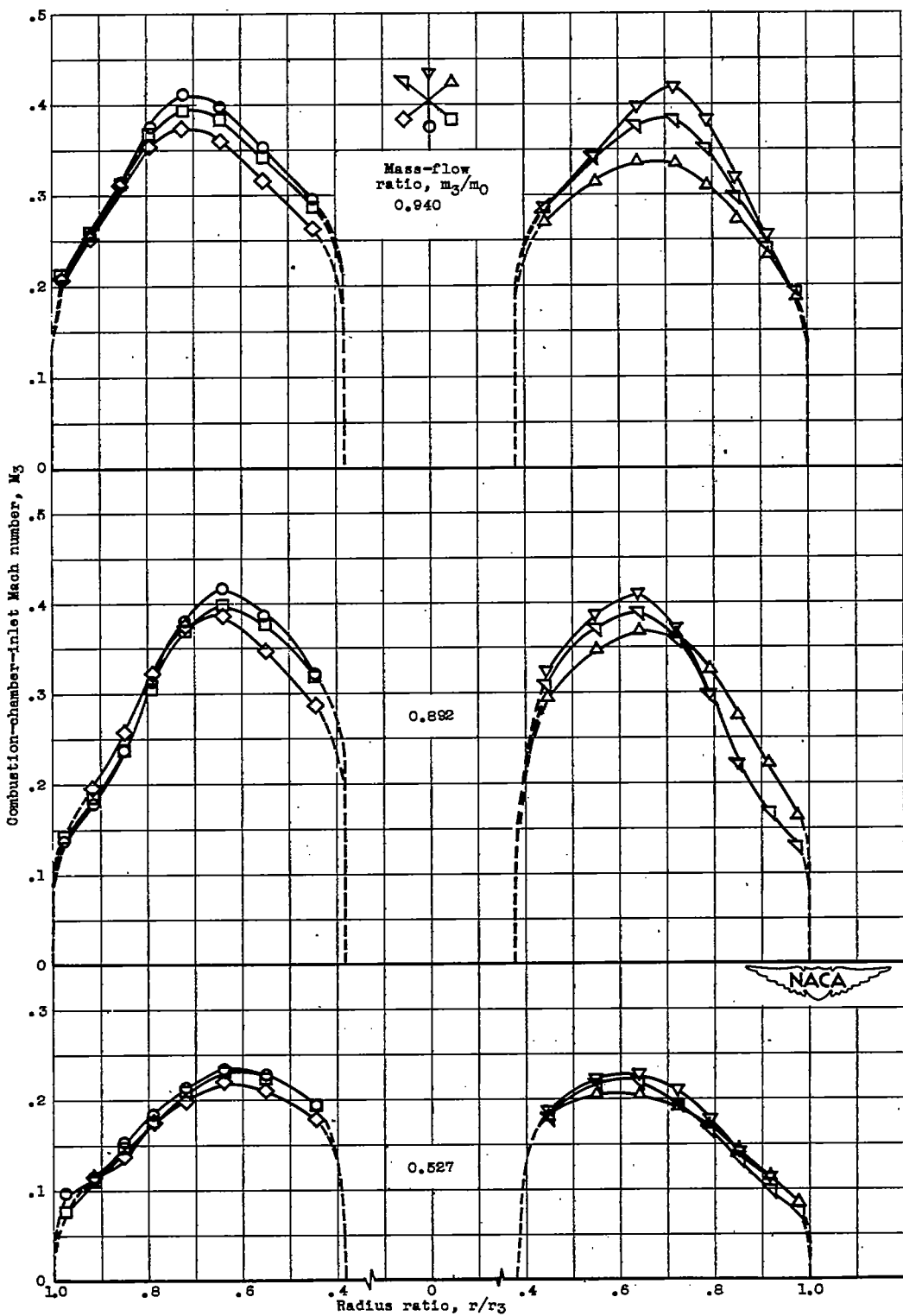


Figure 24. - Variation of Mach number distribution at combustion-chamber inlet for several mass-flow ratios at zero angle of attack. Free-stream Mach number, 1.78.

2039

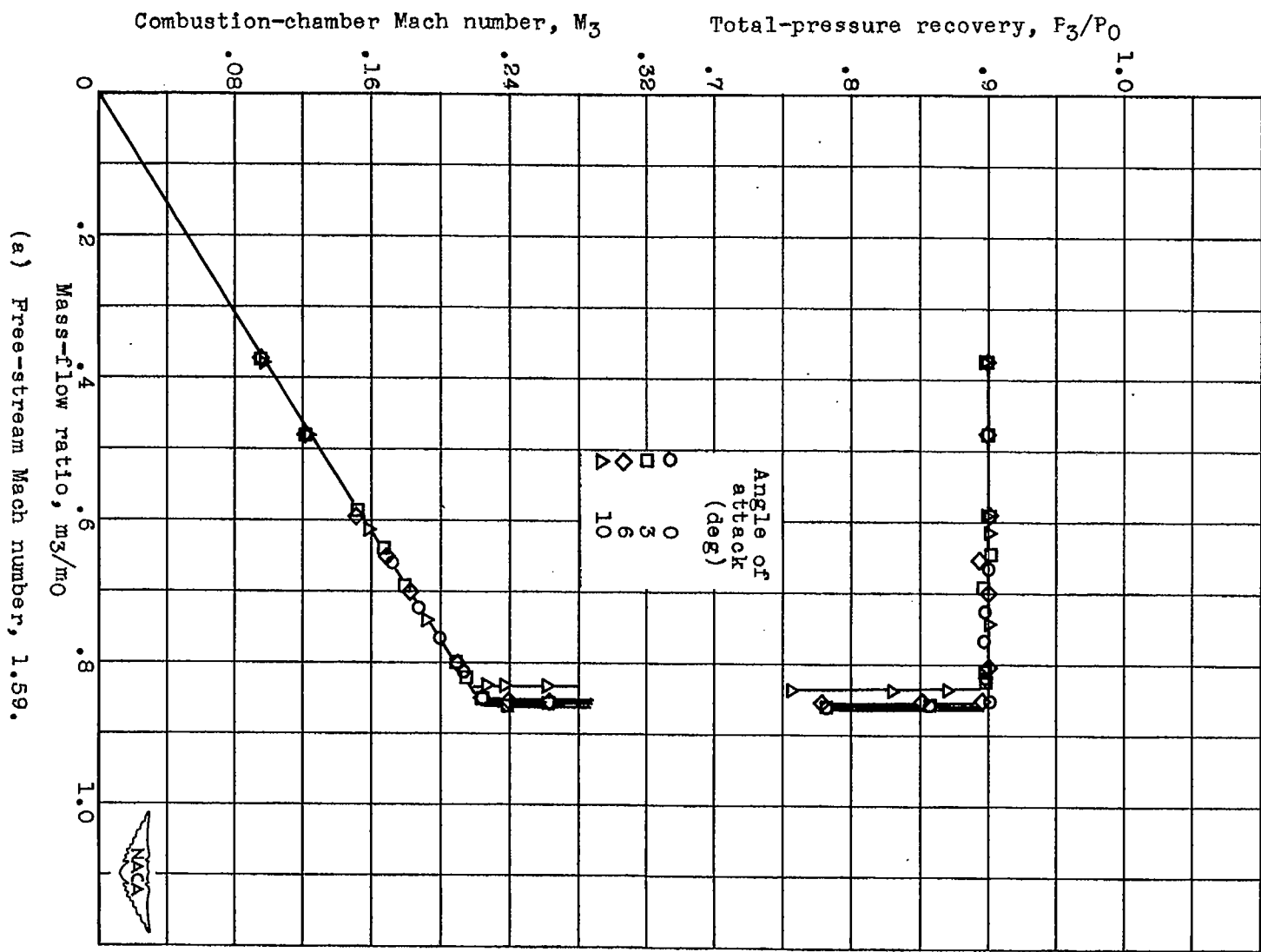
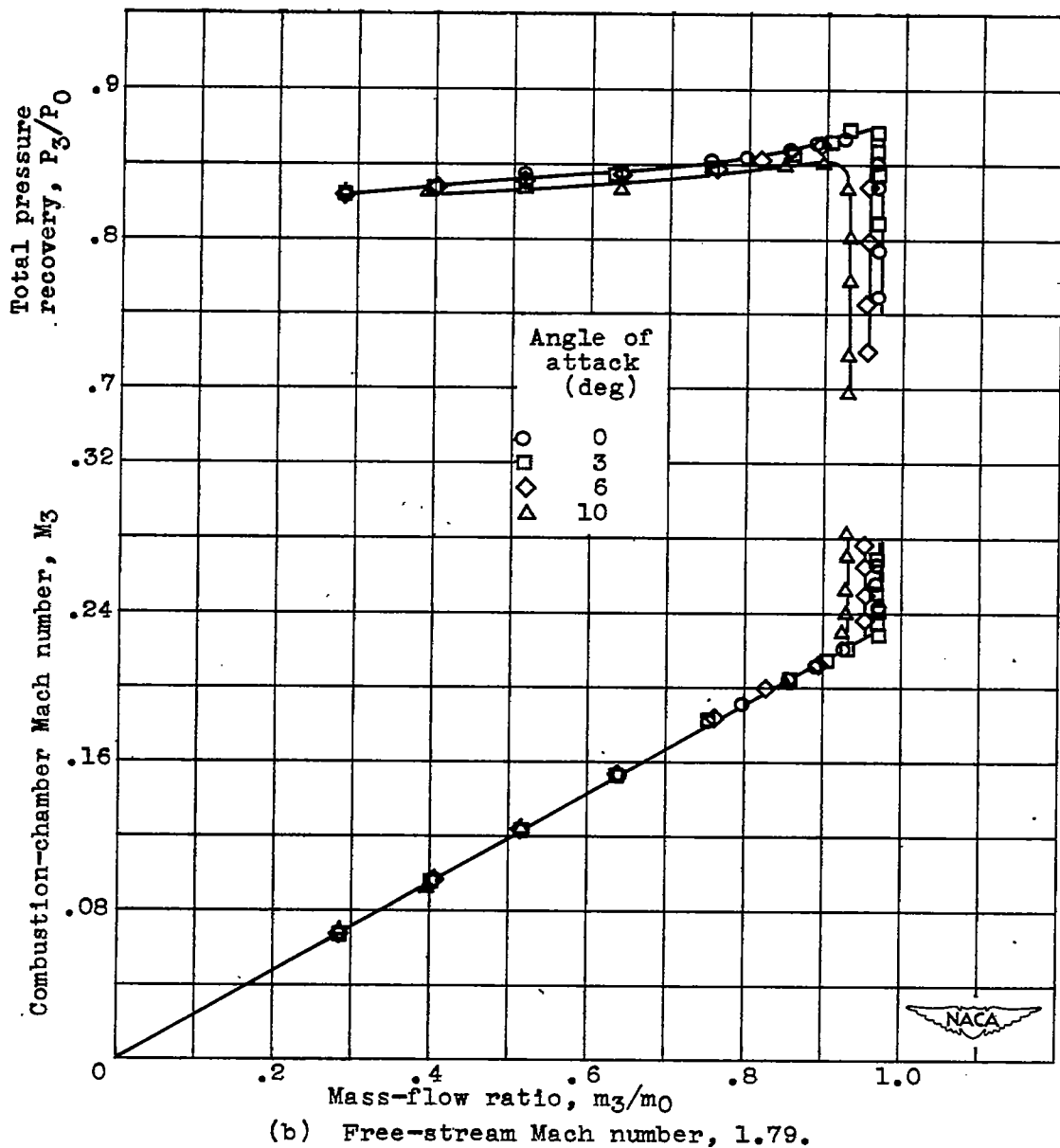
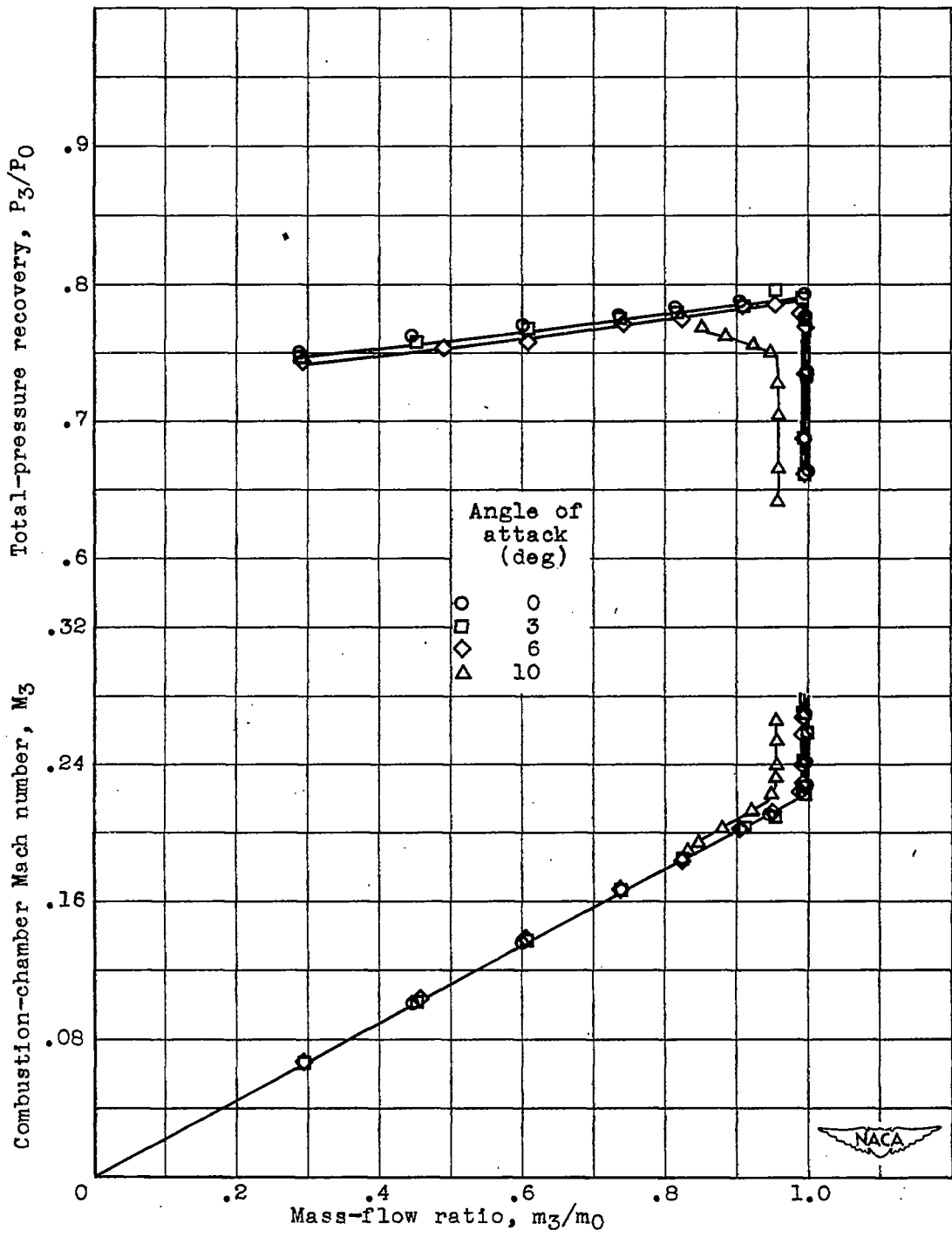


Figure 25. - Variation of total-pressure recovery and combustion-chamber Mach number with mass-flow ratio at four angles of attack for three Mach numbers. Model B.



(b) Free-stream Mach number, 1.79.

Figure 25. - Continued. Variation of total-pressure recovery and combustion-chamber Mach number with mass-flow ratio at four angles of attack for three Mach numbers. Model B.

~~CONFIDENTIAL~~

(c) Free-stream Mach number, 1.99.

Figure 25. - Concluded. Variation of total-pressure recovery and combustion-chamber Mach number with mass-flow ratio at four angles of attack for three Mach numbers. Model B.

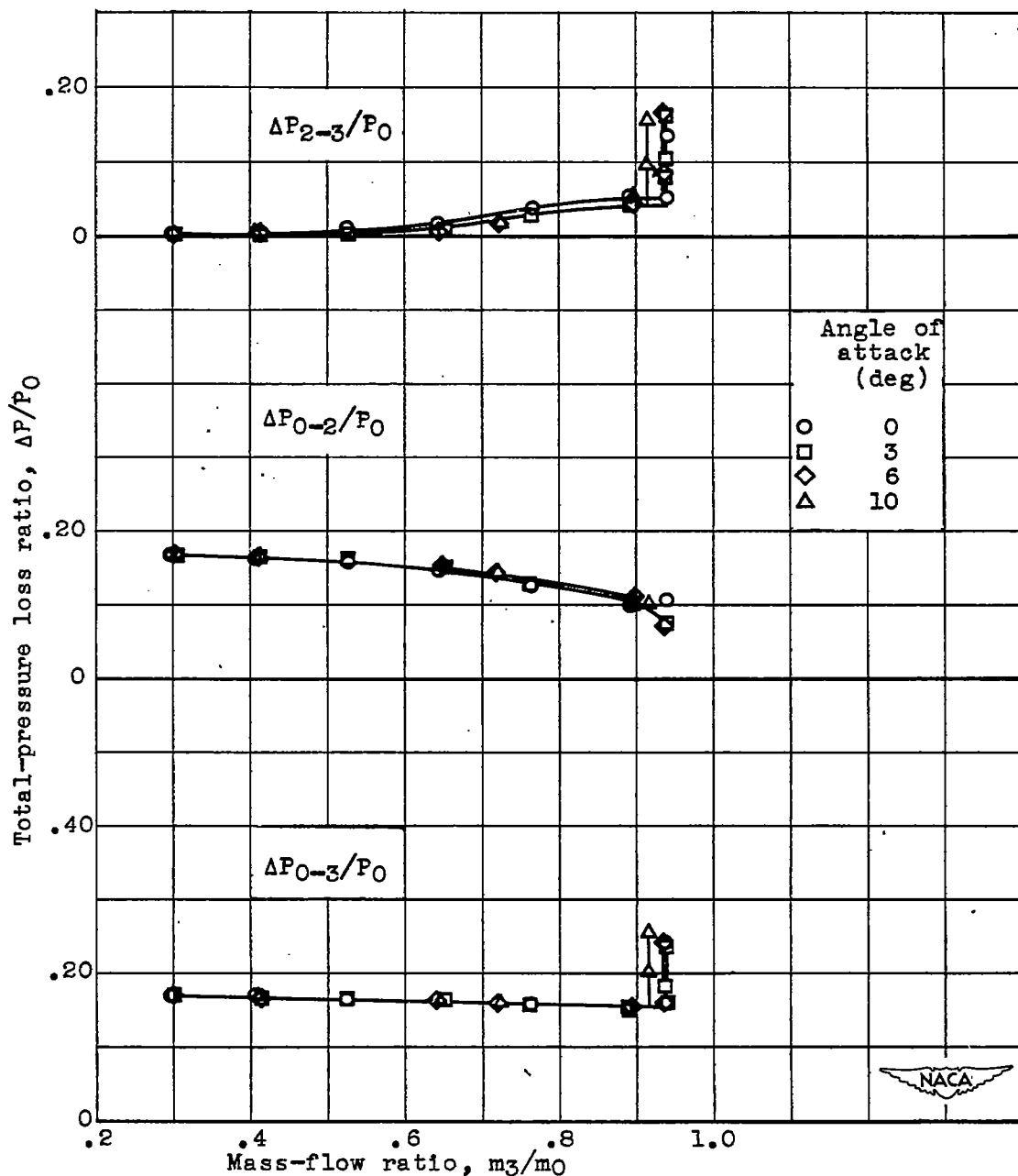


Figure 26. - Variation of inlet and subsonic-diffuser losses with mass-flow ratio at four angles of attack. Free-stream Mach number, 1.79.